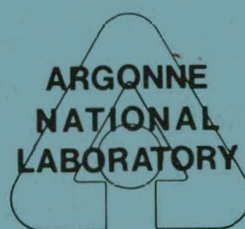


MASTER

TUBE VIBRATION IN INDUSTRIAL SIZE TEST HEAT EXCHANGER

by

H. Halle and M. W. Wambsganss
Components Technology Division



March 1980

DISCLAIMER

This report was prepared as an account of work sponsored by an agency of the United States Government. Neither the United States Government nor any agency Thereof, nor any of their employees, makes any warranty, express or implied, or assumes any legal liability or responsibility for the accuracy, completeness, or usefulness of any information, apparatus, product, or process disclosed, or represents that its use would not infringe privately owned rights. Reference herein to any specific commercial product, process, or service by trade name, trademark, manufacturer, or otherwise does not necessarily constitute or imply its endorsement, recommendation, or favoring by the United States Government or any agency thereof. The views and opinions of authors expressed herein do not necessarily state or reflect those of the United States Government or any agency thereof.

DISCLAIMER

Portions of this document may be illegible in electronic image products. Images are produced from the best available original document.

The facilities of Argonne National Laboratory are owned by the United States Government. Under the terms of a contract (W-31-109-Eng-38) among the U. S. Department of Energy, Argonne Universities Association and The University of Chicago, the University employs the staff and operates the Laboratory in accordance with policies and programs formulated, approved and reviewed by the Association.

MEMBERS OF ARGONNE UNIVERSITIES ASSOCIATION

The University of Arizona
Carnegie-Mellon University
Case Western Reserve University
The University of Chicago
University of Cincinnati
Illinois Institute of Technology
University of Illinois
Indiana University
The University of Iowa
Iowa State University

The University of Kansas
Kansas State University
Loyola University of Chicago
Marquette University
The University of Michigan
Michigan State University
University of Minnesota
University of Missouri
Northwestern University
University of Notre Dame

The Ohio State University
Ohio University
The Pennsylvania State University
Purdue University
Saint Louis University
Southern Illinois University
The University of Texas at Austin
Washington University
Wayne State University
The University of Wisconsin-Madison

NOTICE

This report was prepared as an account of work sponsored by an agency of the United States Government. Neither the United States Government or any agency thereof, nor any of their employees, make any warranty, express or implied, or assume any legal liability or responsibility for the accuracy, completeness, or usefulness of any information, apparatus, product, or process disclosed, or represent that its use would not infringe privately owned rights. Reference herein to any specific commercial product, process, or service by trade name, mark, manufacturer, or otherwise, does not necessarily constitute or imply its endorsement, recommendation, or favoring by the United States Government or any agency thereof. The views and opinions of authors expressed herein do not necessarily state or reflect those of the United States Government or any agency thereof.

TUBE VIBRATION IN INDUSTRIAL SIZE
TEST HEAT EXCHANGER

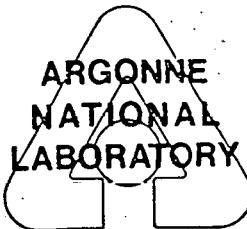
by

H. Halle and M. W. Wambsganss

Components Technology Division

DISCLAIMER

This book was prepared as an account of work sponsored by an agency of the United States Government. Neither the United States Government nor any agency thereof, nor any of their employees, makes any warranty, express or implied, or assumes any legal liability or responsibility for the accuracy, completeness, or usefulness of any information, apparatus, product, or process disclosed, or represents that its use would not infringe privately owned rights. Reference herein to any specific commercial product, process, or service by trade name, trademark, manufacturer, or otherwise, does not necessarily constitute or imply its endorsement, recommendation, or favoring by the United States Government or any agency thereof. The views and opinions of authors expressed herein do not necessarily state or reflect those of the United States Government or any agency thereof.



March 1980

DISTRIBUTION OF THIS DOCUMENT IS UNLIMITED

fmg

TABLE OF CONTENTS

	<u>Page</u>
ABSTRACT	1
I. INTRODUCTION	2
II. TEST DESCRIPTION	4
A. Test Heat Exchanger	4
B. Flow-Induced Vibration Test Facility	4
C. Tube Identification	8
D. Test Configurations	8
III. TEST PARAMETERS/INSTRUMENTATION/DATA PROCESSING	13
A. Flow Rate	13
B. Water Velocity	13
C. Pressure Drop and Level	14
D. Tube Vibrator	14
E. Tube Acceleration and Displacement	15
IV. NATURAL FREQUENCY AND DAMPING	17
A. Full Tube Bundle Configuration	17
B. No-Tubes-in-Window Configuration	22
V. FLOW TESTS	24
A. Full Tube Bundle Configuration	24
B. No-Tubes-in-Window Configuration	43
VI. PRESSURE MEASUREMENTS	46
VII. CONCLUDING REMARKS	49
ACKNOWLEDGMENTS	55
REFERENCES	56
APPENDICES	
A. Principal Test Instrumentation	57
B. Preparatory Test Work	58

LIST OF FIGURES

<u>No.</u>	<u>Title</u>	<u>Page</u>
1	Configuration of test heat exchanger	5
2	Test heat exchanger installation	7
3	End view of test heat exchanger	7
4	Tube layout	9
5	Test heat exchanger in no-tubes-in-window configuration	12
6	Electrodynamic vibrator for internal-to-tube mounting	12
7	Theoretical tube frequencies with water on shell side	18
8	Natural frequency determination via sine sweep, Tube V24	19
9	Typical power spectral density (PSD) curves, Tube V6	31
10	RMS displacement, Tube V6 (full tube bundle, 8 crosspass)	32
11	RMS displacement, Tube V40 (full tube bundle, 8 crosspass)	33
12	RMS displacement, Tube V24 (full tube bundle, 8 crosspass)	34
13	RMS displacement, Tube A23 (full tube bundle, 8 crosspass)	35
14	Principal vibration frequencies, Tube V6 (full tube bundle, 8 crosspass)	36
15	Principal vibration frequencies, Tube V40 (full tube bundle, 8 crosspass)	37
16	Principal vibration frequencies, Tube V24 (full tube bundle, 8 crosspass)	38
17	Principal vibration frequencies, Tube A23 (full tube bundle, 8 crosspass)	39
18	Heat exchanger pressure drop (8 crosspass configuration)	47
19	Tap location and pressure drop distribution	48

LIST OF TABLES

<u>No.</u>	<u>Title</u>	<u>Page</u>
1	General Features and Basic Dimensions of Test Heat Exchanger	6
2	Test Parameters	10
3	Natural Frequencies (f_n) and Damping (ζ_n) of Four Span Tubes	20
4	Natural Frequencies (f_n) and Damping (ζ_n) of Eight Span Tubes	23
5	Flow Tested Tube Bundle/Nozzle Size Combinations	25
6	Test History - Full Tube Bundle	26
7	Critical Flow Rates: Full Tube Bundle	42
8	Test History - NTIW Bundle	45

TUBE VIBRATION IN INDUSTRIAL SIZE

TEST HEAT EXCHANGER

by

H. Halle and M. W. Wambsganss

ABSTRACT

Tube vibration data from tests of a specially built and instrumented, industrial-type, shell-and-tube heat exchanger are reported. The heat exchanger is nominally 0.6 m (2 ft) in diameter and 3.7 m (12 ft) long. Both full tube and no-tubes-in-window bundles were tested for inlet/outlet nozzles of different sizes and with the tubes supported by seven, equally-spaced, single-segmental baffles. Prior to water flow testing, natural frequencies and damping of representative tubes were measured in air and water. Flow testing was accomplished by increasing the flow rates in stepwise fashion and also by sweeping through a selected range of flow rates. The primary variables measured and reported are tube accelerations and/or displacements and pressure drop through the bundle. Tests of the full tube bundle configuration revealed tube "rattling" to occur at intermediate flow rates, and fluidelastic instability, with resultant tube impacting, to occur when the flow rate exceeded a threshold level; principally, the four-span tubes were involved in the regions immediately adjacent to the baffle cut. For the range of flow rates tested, fluidelastic instability was not achieved in the no-tubes-in-window bundle; in this configuration the tubes are supported by all seven baffles and are, therefore, stiffer.

I. INTRODUCTION

Tube vibrations in heat exchangers have plagued industry for years. Flow-induced vibrations have resulted in tube failure due to mechanical wear, fretting corrosion, and fatigue cracking. The detrimental effects of tube vibration failures, including costly plant shutdowns, have motivated numerous investigations. While insights and understanding of basic phenomena are being achieved from laboratory studies, the design criteria developed are considered to be inadequate in predicting flow induced vibration problems in real heat exchangers. As a consequence, the industry is often faced with high unit costs and inefficiencies resulting from the need to resort to overly conservative design to ensure that potential tube vibrations will be avoided. To evaluate and improve prediction methods and design criteria, data obtained under controlled conditions simulating the flow conditions in an actual heat exchanger are required. Furthermore, as an aid to understanding heat exchanger tube vibrations, and to enable further evaluation of existing and new methods for predicting tube vibration, field experience is required from heat exchangers which have experienced failures, and from units which are operating satisfactorily.

The acquisition of tube vibration data was a research recommendation of a 1976 Heat Exchanger Tube Vibration Workshop. The workshop was organized and conducted by Heat Transfer Research, Inc. (HTRI) for the Division of Conservation Research and Technology of the U.S. Energy Research and Development Administration (ERDA). An objective of the workshop was to identify the most promising areas of needed research in flow-induced vibration in industrial shell-and-tube heat exchangers. An international panel of 14 vibration experts, representing ongoing research, presented their evaluation of the state-of-the-art and participated with other attendees in discussions and formulation of research recommendations. The results of the discussions were published by Chenoweth [1].

Based, in part, on the results and recommendations from this workshop, a heat exchanger tube vibration program was established at Argonne National Laboratory (ANL). The objectives are (1) to obtain tube vibration data under controlled conditions from tests of specially built and instrumented, industrial-type, shell-and-tube heat exchangers, (2) to obtain tube vibration data from field experiences collected and subsequently entered into a data bank, and (3) to use the above data to further the understanding of tube-excitation mechanisms and to evaluate and improve current predictive methods and design guidelines. This report is concerned with the first of the above objectives and presents the design, procurement, and initial testing of a test heat exchanger. Efforts to date to establish a tube vibration data bank (the second of the above objectives) are reported in Ref. 2. The data evaluation effort has not been formally started.

This report covers the design and testing of a segmentally-baffled shell and tube heat exchanger. The test heat exchanger is designed to permit ready disassembly and reassembly to obtain the configurations necessary to provide various test parameters affecting tube natural frequency, flow conditions, and tube pattern. The initial configuration, reported herein, consists of eight crosspasses. The test procedure includes determination of the vibration response of the tubes as a function of the shellside, water flow rate. Of particular importance is the investigation of the critical flow rate, at which a fluidelastic instability subjects groups of tubes to large amplitude vibration, impacting, and damage potential. Pressure drop across various regions of the test heat exchanger is also measured. The tape recorded test data are processed, most often by means of spectral analysis for vibration amplitudes and frequency, and tabulated for purpose of subsequent comparison and analysis.

II. DESCRIPTION

A. Test Heat Exchanger

A design study performed with the aid of consultations with Heat Transfer Research, Inc. (HTRI), an applications oriented research organization in the field of heat transfer, resulted in the selection of a nominally 0.6 m (2 ft) diameter, 3.7 m (12 ft) long, test heat exchanger. The initially procured configuration is shown on Fig. 1. Table 1 presents a general description of the shell-and-tube type test heat exchanger. The seven single segmental baffles/eight crosspass arrangement contains three different tube support configurations with four equal spans, five unequal spans, and eight equal spans, respectively.

Upon fabrication, the test heat exchanger was installed and connected to the Flow-Induced Vibration Test Facility (FIVTF) at ANL as shown on Fig. 2. The inlet connection (left center of photo) provides more than 12 diameters of straight pipe to reduce extraneous prior-to-entrance effects. A closeup of the flow exit end is shown on Fig. 3.

B. Flow-Induced Vibration Test Facility

The Flow-Induced Vibration Test Facility has four pumps with flow rates of 0.032, 0.063, 0.16, and 0.25 m^3/s (500, 1000, 2500, and 4000 gpm) at 1.0 MPa (150 psig) discharge pressure. The pumps discharge individually through their own control and by-pass valves, flowmeters and piping (including pressure and temperature indicators) to an accumulator. Thus, the flow can be varied to provide discrete and stable water flow from 0.003 m^3/s (50 gpm) to a maximum of 0.50 m^3/s (8000 gpm) by operating combinations of the pumps and valving. To allow ease of operation by the experimenter, all pumps and valves are operated remotely from the existing data acquisition facility via a control console.

The 30 m^3 (8000 gal) accumulator at the entrance to the test legs has a maximum turnover rate of once per minute at the highest flow rate. This

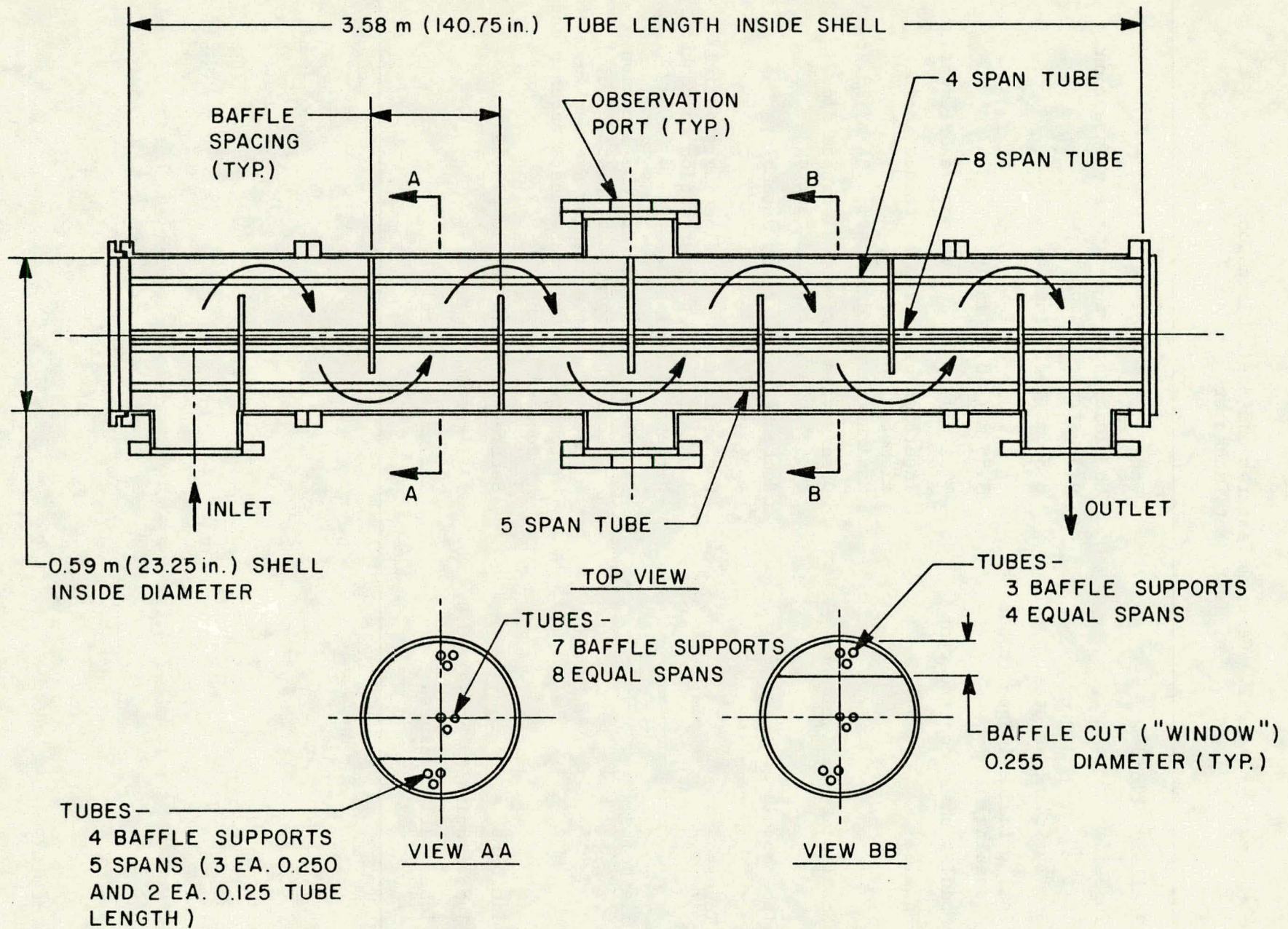


Fig. 1. Configuration of test heat exchanger

TABLE 1. General Features and Basic Dimensions
of Test Heat Exchanger

Shellside fluid	Water
Tubeside	No fluid, open tubes, ready insertion of instrumentation
Shell (Stainless steel), I.D.	0.59 m (23.25 in.)
Shell, inside length (tubesheet spacing)	3.58 m (140.75 in.)
Modular shell construction	Flexibility to change nozzle orientation
Nozzles	Insertion of piping to reduce inside diameter possible Maximum inside diameter: 0.34 m (13.25 in.)
Nozzles at shell midspan	Observation ports or alternate flow route (e.g., direct crossflow)
Tube bundle	Removable unit, ready assembly/ disassembly
Tubesheets	One stationary, one floating; special double tubesheet construction to contain O-rings to seal tubes
Tie bolts	Stainless steel rods in tube locations <ul style="list-style-type: none"> • Secure and space tubesheets on both ends of heat exchanger • Compress double tubesheets on each end to seal O-rings
Tie bars	Secure and space baffle plates
Tube (Admiralty brass), O.D.	19.1 mm (0.750 in.)
Tube, wall thickness	1.2 mm (0.049 in.)

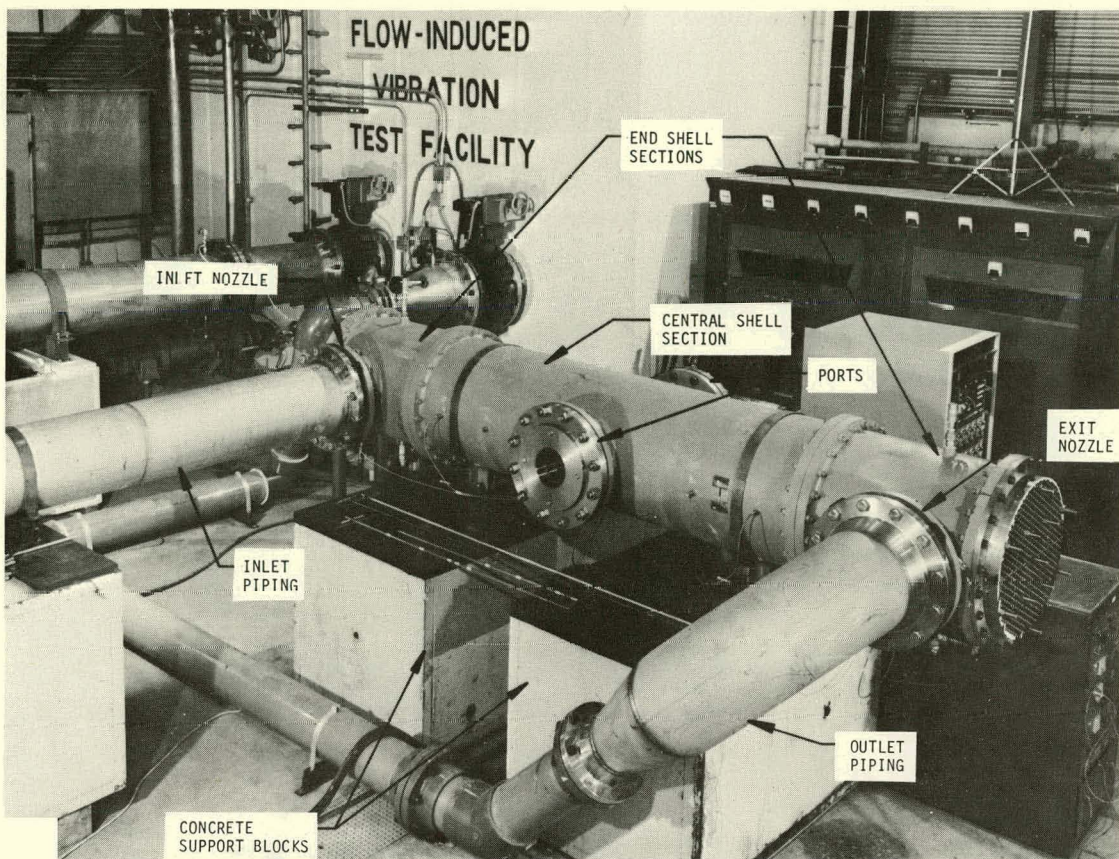


Fig. 2. Test heat exchanger installation

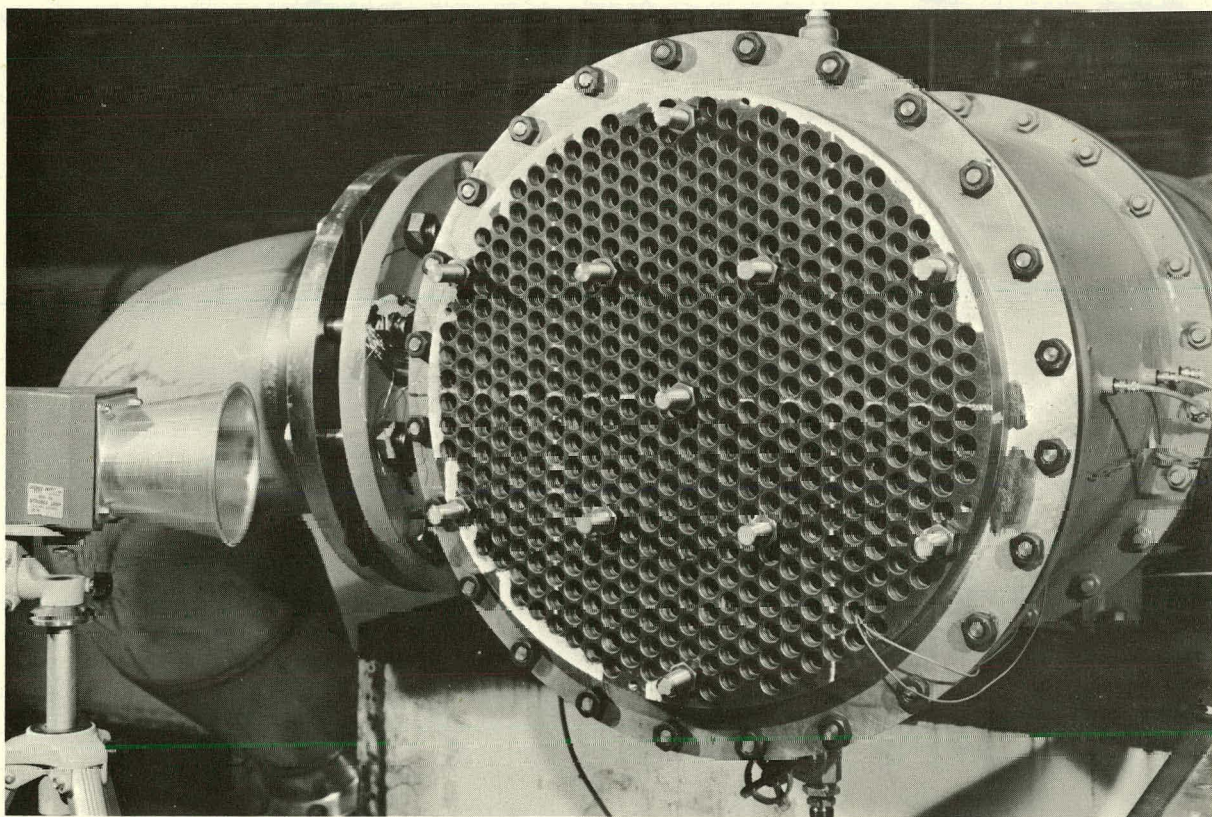


Fig. 3. End view of test heat exchanger

turnover rate, along with internal baffling and the small height-to-diameter ratio, tends to isolate the pump supply from the test item. The pump supply tank is constructed of concrete to reduce vibration and has a large volume ($\sim 38 \text{ m}^3$ (10,000 gal)) to accommodate baffling and water-conditioning equipment. The conditioning equipment is used to maintain the temperature level and resistance of the water so that the transducers for the data acquisition system will not be adversely affected by variable water conditions.

C. Tube Identification

The scheme to identify tube location is illustrated in Fig. 4. The 27 transverse rows are designated by letters from A to AA, and the tubes in any row are numbered, odd or even, from 1 to 47, with number 24 located on the heat exchanger center line.

D. Test Configurations

The different heat exchanger configurations to be tested are characterized by combinations of various parameters. Table 2 presents these parameters for the tests performed to date and also for future tests, which eventually will require new tubesheets, new baffles, and/or reorientation of inlet/outlet nozzles. As the program proceeds, the most promising parameter combinations will be selected to be tested. Possible future developments of tube vibration prevention designs will also be considered.

This report covers all testing performed with the eight crosspass, seven uniformly spaced baffle configuration. A full tube bundle was tested with all three, and a no-tubes-in-window (NTIW) bundle with two, of the inlet/outlet diameter nozzles listed.

For the full tube bundle configuration, it is seen from Fig. 4 that the four span, five span, and eight span tubes, are located in rows V through AA, A through F, and H through T, respectively. Since the baffles are cut along the centerline of rows U and G, the tubes in these rows have a special

- TUBE WITH SIGNIFICANT VIBRATION
- TIE BOLT (11 LOCATIONS)
- TIE BAR (8 LOCATIONS)

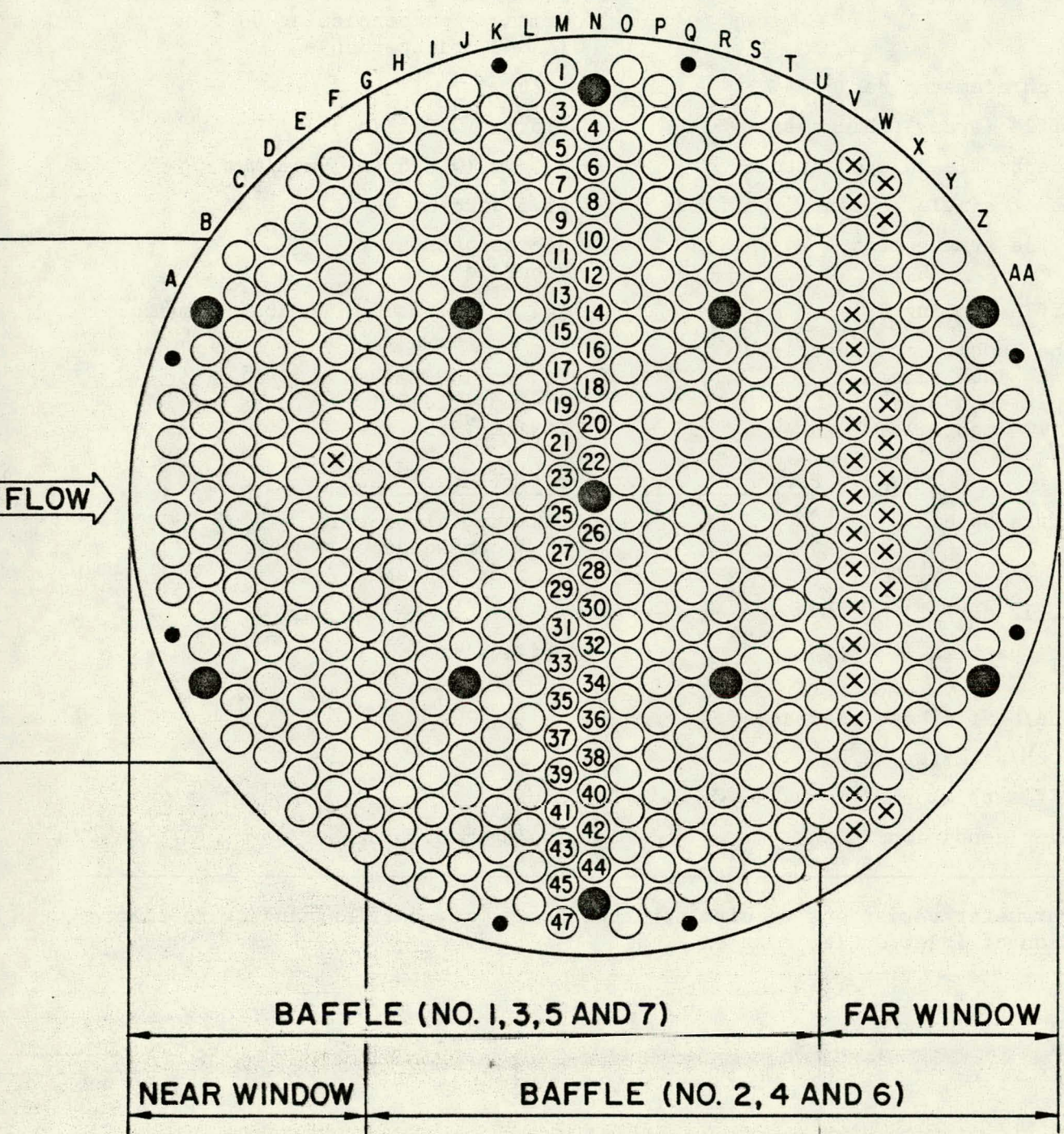


Fig. 4. Tube layout

TABLE 2. Test Parameters

<u>A. Parameters for Initial Set of Tests</u>	
Tube pattern	Triangular, one side of equilateral triangle perpendicular to flow ("30°" orientation)
Pitch/diameter ratio	1.25
Baffle (brass) thickness	9.5 mm (0.375 in.)
Tube/baffle hole clearance	0.4 mm (0.016 in.) minimum
Cut of single segmental baffles	25.5 percent
Baffle arrangement	8 crosspasses 7 baffles
Baffle spacing	444 mm (17.5 in.) nominally uniform
Tube bundle configurations	
14 inch size	337 mm (13.25 in.)
12 inch size	289 mm (11.38 in.)
10 inch size	243 mm (9.56 in.)
<u>B. Parameter Variations for Future Tests</u>	
Baffle spacing	Uniform; asymmetric 6, 4 crosspasses* 7, 5 crosspasses*
Baffle cut	
Tube pattern*	Triangular (60°) Square (45°, 90°)
Tube/baffle hole clearance*	
Pitch/diameter (P/D)*	
Baffle thickness*	
Inlet conditions*	Impingement plates

*Parameter variations require new tubesheets, new baffles, and/or reorientation of inlet/outlet nozzles.

saddle type support which provides a "one-way" four or five span configuration, respectively, in the plane of the alternating flow around the baffles. In all other directions, these tubes are generally supported by all seven baffles; however, it should be noted that flow direction displacement can alter transverse-to-flow support.

The NTIW configuration was obtained by removing all five and four span tubes in rows A to F and V to AA, respectively. The saddle rows G and U were left in place. To prevent leakage, the unused tubesheet and baffle plate holes had to be sealed or covered, respectively. Fig. 5 shows the NTIW bundle on a specially built transporter prior to insertion into the shell and prior to the assembly of additional external back-up plates (seen on Fig. 3) to strengthen the tubesheets for satisfactory O-ring sealing.

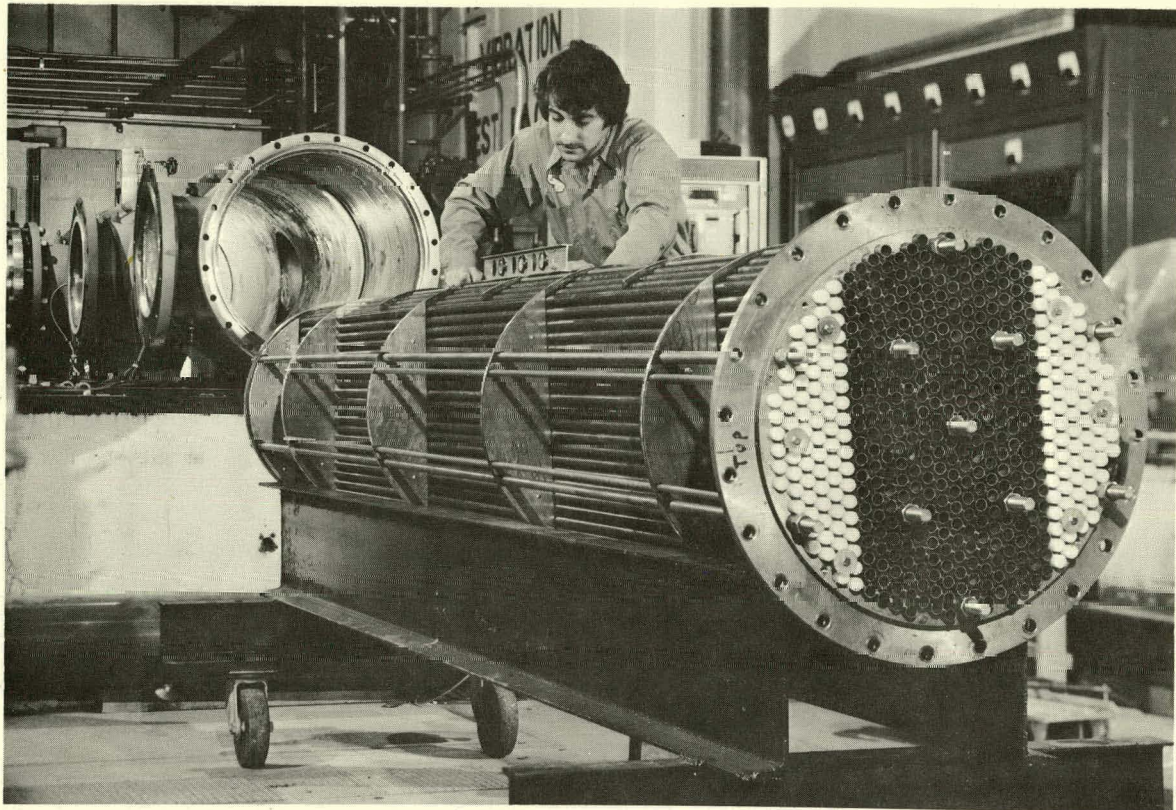


Fig. 5. Test heat exchanger in no-tubes-in-window configuration

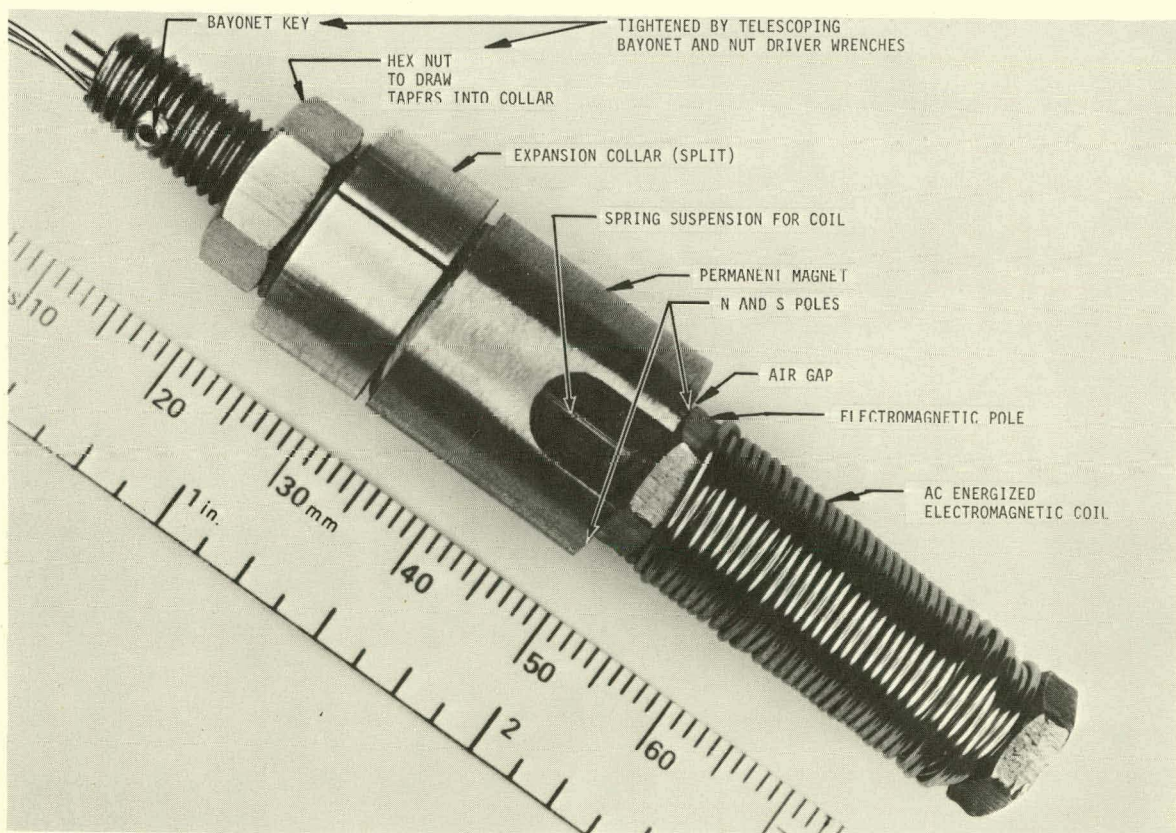


Fig. 6. Electrodynamic vibrator for internal-to-tube mounting

III. TEST PARAMETERS/INSTRUMENTATION/DATA PROCESSING

The principal test parameters which characterize the flow conditions and structural response of the heat exchanger are presented below. Also described are the measurement methods, instrumentation, and data processing employed to acquire these parameters. Specific instrumentation items utilized are listed in Appendix A.

A. Flow Rate

The water flow rate through the test heat exchanger was measured with turbine flowmeters. Each of the four pumps in the loop is equipped with an individual meter. Signal pulses from the flowmeters are recorded on tape and are usually converted to d.c. voltages by means of a rate indicator to facilitate the subsequent data analyses.

B. Water Velocity

The crossflow velocity in the gap between the tubes is one of the most significant parameters influencing the vibration performance of a heat exchanger. However, measurement of the magnitude and direction of this gap velocity requires accessibility, evaluation to determine the mean transverse-to-tube velocity within a gap, and analysis of measurements taken at various locations in the test heat exchanger. Substantial instrumentation problems would have to be overcome. The introduction of physical probes will affect the flow pattern within the gaps. The use of unobtrusive laser anemometry requires visual access. The use of ultrasonic techniques or other methods (for example, measuring the time delay of signal between two stations) could probably be developed; however, the effort required for such development and calibration was considered to be beyond the scope of the present program.

For the present analysis, the crossflow velocity is computed from the overall flow rate through the heat exchanger by means of the HTRI computer program ST-4. The calculation is influenced by the flow diverted from the

subject tube gaps due to leakage through various bypass paths: around the tube bundle, and through tube/baffle hole and baffle/shell clearances. These leakage flows depend on the pressure drops experienced across the various internal sections of the heat exchanger. The measurement of such pressure drops is part of this test work.

C. Pressure Drop and Level

As mentioned above, the knowledge of pressure drops between various sections of the heat exchanger provides input to computer programs. Pressure taps are provided at the inlet, the outlet, the center nozzle and at six longitudinal locations on the surface of the shell in the horizontal plane. The pressure taps (which can be seen on Figs. 2 and 3) are connected with tubing via a manifold and valves, as appropriate, to a differential pressure transducer to determine the pressure difference to the heat exchanger outlet or the central tap.

The gage pressure of the heat exchanger outlet was measured by means of a differential pressure transducer. In addition, a strain gage pressure transducer was installed flush with the internal shell surface in the region of the first turnaround. This pressure transducer had sufficient frequency response to measure pressure fluctuations.

D. Tube Vibrator

An internal tube vibrator was developed to provide vibration excitation of an installed tube by means of sine sweep frequency tests for the determination of (1) the fundamental as well as the higher natural frequencies and (2) damping at constant, though moderate, amplitude levels. As shown on Fig. 6 the vibrator features a magnet coil which is spring suspended in the field of a permanent magnet. Alternating current of controlled magnitude and frequency drives the coil into vibration. The reaction force between the coil support and tube provides a forced excitation. The entire assembly

can be located and secured deep inside a 16.6 mm (0.652 in.) I.D. tube by means of a split collar that is expanded against the internal tube wall by means of a nut and tapered surfaces. Coincidence of the vibrator frequency with one of the tube natural frequencies excites the tube to moderate vibration levels.

E. Tube Acceleration and Displacement

Tube response was generally measured by means of miniature accelerometers placed on special mounts inserted through the open ends of the tubes. The longitudinal location in the tube was chosen to provide optimum amplitude response to fundamental (first) mode vibration. The initially used rigid accelerometer mounts were secured to the tube (by the method also used for the vibrator, see Fig. 6) and the accelerometers were attached by a suitable adhesive, usually dental cement. This accelerometer/mount combination provided high frequency response and functioned properly as long as no impacting of tubes occurred. However, upon tube impacting there were two detrimental effects: (1) the noise generated by the high frequency signals saturated the electronics and rendered signal processing futile and (2) the impact forces caused a number of the delicate accelerometers to be shaken loose from their mounts and to be severely damaged from bouncing against the tube-walls.

Test work with the full tube bundle indicated that the vibration frequencies of practical significance were less than 60 Hz. To reduce or eliminate the above problems it was decided to cushion the accelerometers in foam mounts that would mechanically filter the high frequency accelerations and prevent damage. Prior to installation, the accelerometer/mount assemblies were tested on a small test shaker and transfer functions were obtained utilizing a standard accelerometer. The lowest natural frequency of the accelerometer/mount combination was 400 Hz or more, and the response

was practically linear to 100 Hz. For the subsequent testing of the stiffer NTIW configuration, accelerometer mounts utilizing a rigid foam plastic were developed and comparison tested to provide a valid frequency response to 400 Hz.

A fast Fourier transform (FFT) spectrum analyzer was employed to obtain power spectral density (PSD) curves from the acceleration signals. Each acceleration PSD was divided by a function proportional to the fourth power of the frequency to obtain the corresponding displacement PSD. Subsequently, the rms value of the displacement was obtained by taking the square root of the area under the integral of the PSD curve with respect to frequency within the bandwidth under consideration.

In order to make unobtrusive displacement measurements through the entire range of tube vibration, an optical bi-axial displacement follower system was procured and used on a selected tube during the last test runs with the full tube bundle. Additionally, high speed motion pictures were taken of vibrating tubes.

IV. NATURAL FREQUENCY AND DAMPING

In theory, the tubes are modeled as straight beams, rigidly clamped at the ends with intermediate, perfectly aligned, frictionless, pivoted supports. In practice, the tubes are slightly bowed, usually bearing against the internal wall of the oversize (clearance) holes in the baffle plates. Focusing initially on the full tube bundle, Fig. 7 presents the results of a theoretical calculation [3] of the natural frequencies and mode shapes of ideal four and five span tubes in still water for the first six modes. The frequencies are based on an added mass correction factor of 2.97 which takes into account the proximity to surrounding tubes in the tube bundle.

Natural frequencies of the tubes were determined by two different methods: (1) a specially developed electrodynamic vibrator (Fig. 6), mounted internal to the tube and excited to provide a sine sweep through the frequency range of interest - the resulting accelerometer response is plotted as a function of frequency; and (2) impact excitation (usually a mallet blow struck against the external shell surface) - the transient acceleration response is captured and processed for frequency content on a frequency spectrum analyzer. These tests were performed in air (i.e., with an empty heat exchanger) and with the heat exchanger filled with still water. The direction of vibration excitation and sensitivity of the accelerometers was usually transverse to the plane of the subsequent flow.

A. Full Tube Bundle Configuration

Typical frequency response curves for the excitation of tube V24 in air and water are given on Fig. 8. In Table 3 test data for two typical four-span tubes, V24 and AA23, are presented. Only the principal frequencies are listed in Table 3. It should be noted, as can be seen from Fig. 8, that other frequency peaks are also present. As indicated above, the theoretical

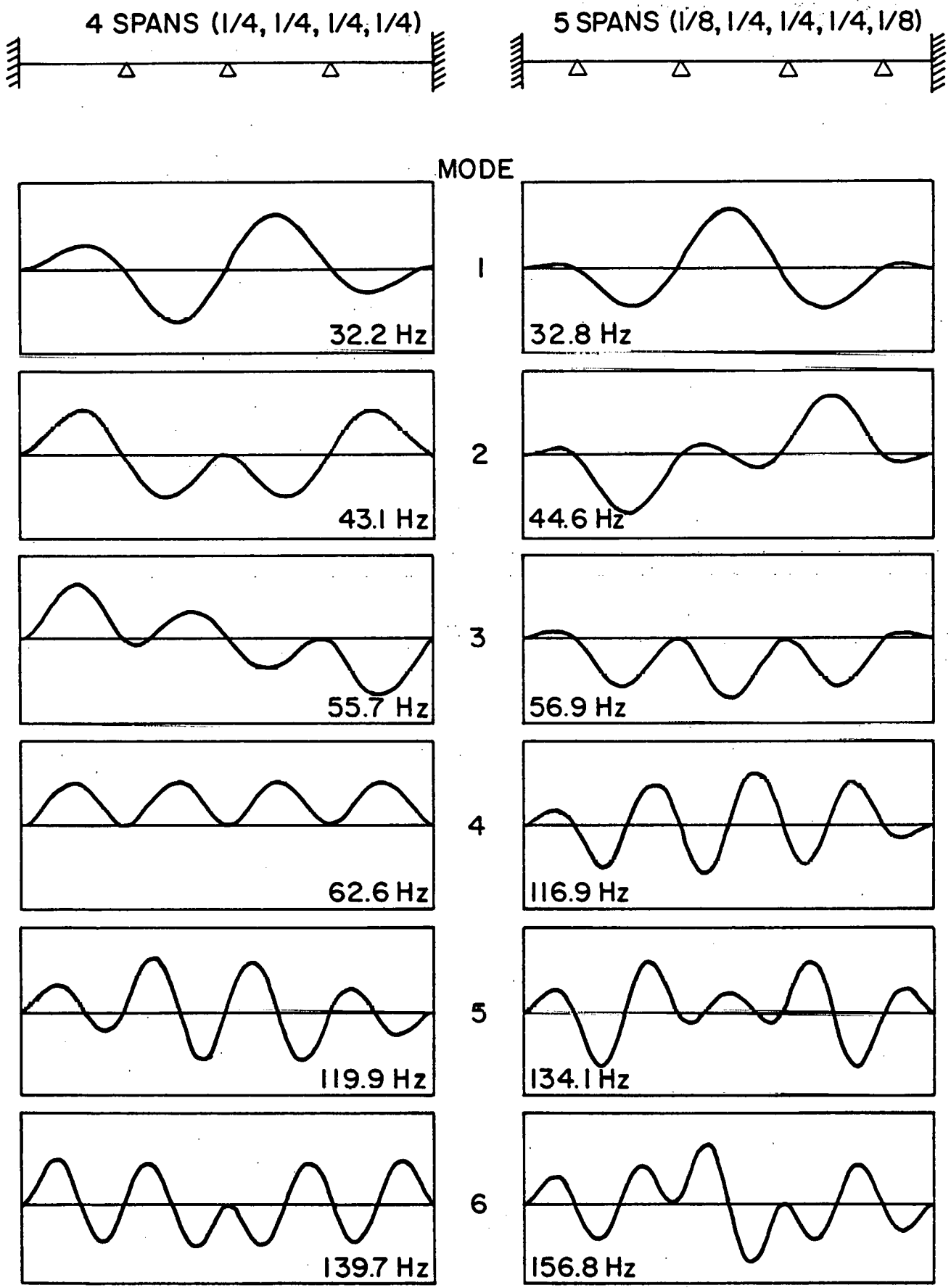


Fig. 7. Theoretical tube frequencies with water on shell side

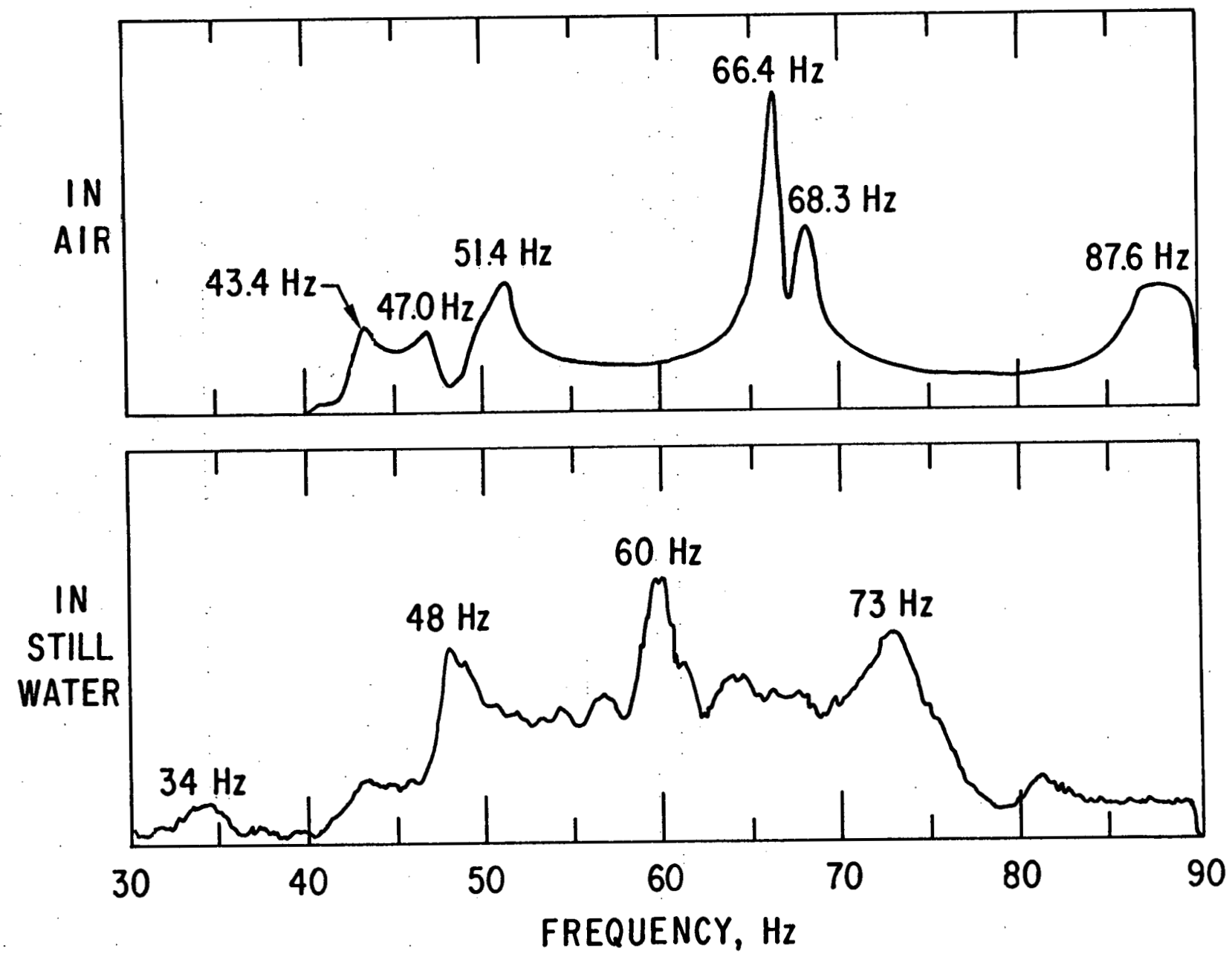


Fig. 8. Natural frequency determination via sine sweep, Tube V24

TABLE 3. Natural Frequencies (f_n) and Damping (ζ_n) of Four Span Tubes

Mode n	(f_n) _{air} , Hz			(ζ_n) _{air}		(f_n) _{water} , Hz			(ζ_n) _{water}	
	Theory	V24	AA23	V24	AA23	Theory	V24	AA23	V24	AA23
1	50.1	51	51	0.018	0.088	32.2	34	44	0.033	0.015
2	67.0	66	62	0.007	0.048	43.1	48	59	0.035	0.031
3	86.6	87	79	0.021	0.019	55.7	60	70	0.018	0.033
4	97.3		94		0.007	62.4	73	77	0.028	0.013
5	186.3	182	187	0.019		119.9	118	130	0.021	0.027
6	217.2	218	212	0.009	0.006	139.7	152	180	0.014	0.019
7	250.7	252	240	0.005		161.3	168	193	0.027	0.014
8	268.2		263		0.002	172.5	198	214	0.015	0.014

values in water are computed assuming an added mass factor of 2.97, which accounts for the proximity of adjacent tubes internal to the bundle. Tube AA23 is on the periphery of the bundle and would be expected to have a smaller added mass factor and hence higher natural frequencies in water than the theoretical predictions and measured values for tube V24; this is the case as shown in Table 3. Tube AA23 in air gave the clearest results, more than eight modes could be observed at times. Other four-span tubes (e.g., V24) did not respond as well. For a tube "saddled" in the baffle cut row and for a five span tube, the situation was not as clear, as some of the expected lower mode frequencies were not distinctively excited; in effect the "saddled" tube responded like an eight span tube as noted further below.

Even though the support conditions are not perfect, and some coupling with adjacent tubes and supports is no doubt present, the natural frequency determination tests of several four span tubes in air indicated, to varying degrees, reasonably good agreement with theoretical values. This implies that the assumption of knife-edge supports at the baffles is reasonable and agrees with the conclusion of other investigators [4,5].

In water the natural frequency determination of any tube was complicated by the vibration coupling with neighboring tubes. Theoretically, if there are k interacting tubes, there will be $2k$ coupled mode frequencies corresponding to each frequency of a single tube [6]. Upon testing a limited number of frequencies were prominent; for example, see the in-water response curve in Fig. 8. For a given tube the coupling could be attenuated by loading the surrounding tubes to decrease their natural frequency and locally detune the bundle. However, it was not possible to identify the individual mode frequencies, partly because these frequencies are located fairly close together (in groups of four for the four span tube) on the

frequency spectrum. Even among the four span tubes there were differences depending on the location: whether the tube was saddled in the baffle, located on the periphery, or in the internal region of the bundle. For example, as expected, and as shown in Fig. 8, the natural frequencies for tube V24, completely surrounded by other tubes, were lower than for tube AA23, at the periphery of the bundle.

Damping, as expressed by the equivalent viscous damping ratio, ζ , was determined, where possible, from the frequency response curves using the bandwidth method. Typical results for tubes V24 and AA23 are given in Table 3. Because of uncertain factors such as (a) deviation from viscous assumptions, (b) presence of nearby natural frequency contributions, (c) amplitude dependence, and (d) probable operational alteration due to water flow and tube vibration effects, these damping data should be used with discretion.

B. No-Tubes-in-Window Configuration

In general, the above presentation is also applicable to the subsequent natural frequency testing of the NTIW configuration containing only eight span and saddled tubes. Table 4 presents theoretical and experimental data for internal-to-the-bundle, eight-span tubes T24 and H24, and for the saddled tube U5, located on the periphery and corner of the bundle. Again the higher in-water frequencies of the latter peripheral tube are evident. By examining the phase difference between the vibration exciter voltage input and accelerometer signal output some differentiation between odd and even vibration modes was possible. Damping determination was possible only in a few instances.

TABLE 4. Natural Frequencies (f_n) and Damping (ζ_n) of Eight Span Tubes

Mode n	(f_n) air, Hz				(ζ_n) air			(f_n) water, Hz				(ζ_n) water		
	Theory	T24	H24	U5	T24	H24	U5	Theory	T24	H24	U5	T24	H24	U5
1	179	190	175	182	0.009	0.017	0.009	115	110	119	134	0.037	0.022	
2	200			200			0.011	121	121		152	0.020		
3	231	240	242	249				149	151	154	170			
4	268	263	285	289				173	176	171	193			

T24, H24 - Internal Tubes

U5 - Saddled Tube on Periphery

V. FLOW TESTS

A. Full Tube Bundle Configuration

The eight crosspass, full tube bundle heat exchanger was flow tested with three different inlet/outlet nozzle diameter configurations, designated Cases 1-3 and included in the listing on Table 5. Except for visual observation, it was not practically possible to monitor the vibration performance of all 488 tubes. Consequently, only a few of the tubes were selected to be instrumented. Since experience (confirmed by the test results) indicated that the four span tubes were the most susceptible to vibrate, most of the available instrumentation was mounted within these tubes. Location of the instrumentation was changed from time to time; improvements were instituted as the tests proceeded. Up to eight miniature accelerometers were used. A conventional accelerometer was installed on the shell (near pressure tap "B") and another one on the tie bolt in location Z14, sensitive in the axial direction. All accelerometer as well as the flowmeter and timing signals were cabled to FM or PCM recording channels. The tests were performed in two different ways: (1) a constant flow rate level was established and the instrumentation signals were recorded for a time sufficient for subsequent frequency and amplitude analysis, (2) the flow rate was varied (scanned) through a range to determine the flow rate at the initiation and termination of (a) rattling and (b) fluidelastic instability.

The test history on Table 6 lists the principal full tube bundle flow test runs conducted for this program. After some initial trials, the general test sequence was to increase the flow rate stepwise from run to run until the instability was reached and then to perform a scan with a maximum velocity at or slightly above the critical in order not to disturb the tube bundle support conditions. The recorded data were analyzed and studied. To investigate the repeatability of the data, and to gain confidence

TABLE 5. Flow Tested Tube Bundle/Nozzle Size Combinations

Case	Nozzle Size, Nominal Pipe Size, Description	Nominal (Average) Inside Diameter, m (in.)	Average Nozzle Entrance Velocity per 0.0631 m ³ /s (1000 gpm)	Used for Test Runs:
			m/s (ft/sec)	
1	14 in., Schedule 30, nozzles attached to shell during fabri- cation	0.337 (13.25)	0.709 (2.33)	1-29
2	12 in., Schedule 80, inlet/exit inserts	0.288 (11.328)	0.970 (3.18)	30-43
3	10 in., Schedule 80, inlet/exit inserts	0.241 (9.500)	1.38 (4.53)	44-55
4	10 in., Schedule 80, inlet/exit inserts	0.241 (9.500)	1.38 (4.53)	1-14
5	14 in., Schedule 30, (no inserts)	0.337 (13.25)	0.709 (2.33)	15-27

Cases 1-3: Full Tube Bundle

Cases 4 and 5: No-Tubes-In-Window Configuration

TABLE 6. Test History - Full Tube Bundle

Test Date 1979	Case	Run No.	Flow Rate (gal/min)	Comments
-	1	-	various	Instability at 3230
5/7		1	2400	
		2	2790	
		3	3230	
5/8		4	3190	Repeat Run 3
		5	Scan	Twice in and out of instability at 3250
5/18		6	760	Initiated use of dynamic pressure transducer
		7	1200	
		8	1610	
		9	-	Flow changed from 2000 during run
		10	2180	
		11	2390	
		12	2590	
		13	2790	
		14	Scan	2400 - 2800 - 1000
6/8		15	830	
		16	1210	
		17	1610	
		18	Scan	790 - 1850 - and down
		19	Scan	1620 - 2800 - and down
		20	1970	
		21	2410	
		22	2790	
		23	3140	
		24	Scan	In and out of instability near 3250
		25	Scan	In and out of instability near 3250
6/25	-	Misc.		Demonstration, 5 span tube impacting at 3600
7/6		26	2920	Noisy loop
		27	2920	Repeat Run 26
		28	Scan	Investigated instability of 5 span tubes, tested to 3620

TABLE 6. Test History - Full Tube Bundle (Contd.)

Test Date 1979	Case	Run No.	Flow Rate (gal/min)	Comments
		29	Scan	Investigated instability of 5 span tubes, tested to 3910
		-	2000 and 2800	Investigated nozzle flow with pitot tube
		-	3300	High speed movies, V24 region
		-	3380	High speed movies, V6 region
7/24	2	30	1030	
		31	1390	
		32	1800	
		33	2210	
		34	2590	
		35	2780	
		36	3000	
		37	3190	Started impacting during run
		38	Scan	1900 - 3500 - 2000
9/5		39	2010	Started use of cushioned accelerometer mounts
		40	2420	
		41	2760	
		42	3000	
		43	Scan	2500 - 3750 - 2500, instability at 3250
9/19	3	-	800	
		44	1200	
		45	1580	
		46	2010	
		47	2400	
		48	2780	
		49	3000	
		50	Scan	3000 - 3130 - 2000, instability at 3130
10/8		51	2010	
		52	2400	
		53	2810	
		54	3000	
		55	Scan	3000 - 3760 - 1900, instabilities and hysteresis

in the results, on a later date some of the previous tests were repeated and an additional scan or two were performed to a flow level well above the critical.

In general, as the flow rate is increased, the amplitude of tube vibration increases moderately; at intermediate flow rates the tubes can be heard to rattle; and at a critical flow level a fluidelastic instability is abruptly initiated. Principally, the four span tubes are involved. The test results indicate that the primary contribution to the vibration response is from the frequency range from 30 to 60 Hz. However, at high flow rates resonant frequencies in the range of 32 to 38 Hz are usually dominant.

Rattling is audible at intermediate flow rates. As flow rates are increased beyond half of the critical value for instability, the accelerometers begin to show superimposed high frequency impulses; it appears that initially these impulses occur occasionally. At higher flow rates the impulses usually occur periodically at the tube vibration frequencies. It is surmised that the rattling is caused by tube movement and contacting in the baffle clearance holes. Since the noise is transmitted throughout the structure, it is not possible to determine at which of the many tube/baffle-hole combinations the tubes are rattling, nor by what dynamic behavior it is characterized.

The onset of fluidelastic instability can readily be detected by the abrupt increase in noise coming from the exchanger. Large amplitude motion of the tubes result in tubes impacting with one another. Direct identification of impacting tubes by means of the accelerometers was not possible because the impacts are transmitted through the structure and are indicated as high frequency noise even on accelerometers in tubes that may not have impacted. However, at times more than 25 tubes were shaken severely enough to slide and move axially in their O-ring seals, thereby providing a reasonably

good indication where the most severe "action" took place. As shown on Fig. 4, the tubes most strongly subjected to the instability were located (a) in the regions where the baffle cut meets the shell and (b) in row V next to the row saddled in the baffle cut. Usually, the heat exchanger was not permitted to remain more than 30-60 seconds at a time in the instability condition to reduce the potential of damage.

During the Case 2 tests the rigidly mounted accelerometers were replaced by cushioned ones as discussed in Section III.E. However, by reducing high frequency response signals, the ability to detect rattling was also reduced. Nevertheless, the high frequency accelerometer mounted on the shell clearly picked up the rattling; for a spot check the signal was fed into an audio speaker and the rattling could readily be heard.

Even though the instrumented tubes had generally similar response trends, the performance of individual tubes was apparently indicative of their support characteristics. Under ordinary test conditions the O-ring seals held the tubes in place; however during the violent impacting, occurring as the result of fluidelastic instability, many of the affected tubes moved axially and rotated. In some cases these tubes may not have been restored to exactly the initial support conditions prior to the next test. Consequently, the vibrational characteristics of individual tubes can be expected to vary slightly from run to run as well as within a given run. These variations could be expected to show up in the frequency response curves.

Four tubes that were monitored during most of the test runs are the four span tubes V6, V24, and V40, located in the row next to the row saddled in the baffle cut, and five span tube A23, located in the first row exposed to the inlet flow. In the longitudinal direction, the accelerometers were located as follows: in the row V tubes, at approximately the center of the first span from the inlet (V24 and V40) or outlet (V6); in tube A23, midspan

of the second turnaround from the inlet. The accelerometers were oriented to be sensitive in the transverse-to-flow direction. Other tubes instrumented during some of the tests included F6, F22, V22, W7, and AA23.

Typical PSD curves of acceleration and displacement for tube V6 (Case 2, Run 34) are shown in Fig. 9. As discussed in Section III.E, displacement response is obtained by a double integration technique encompassing the bandwidth of 11.8 to 100 Hz; no significant accelerations were measured below 24 Hz. However, because of the inverse to the square of frequency influence of the double integration process, general noise or low level acceleration could contribute significantly to the calculated displacement response, particularly when flow and excitation levels are low or when acceleration response is broadband with few distinguishable frequencies.

RMS amplitudes are computed by integration of the PSD curves. In Figs. 10-13 typical curves of rms response, nondimensionalized by tube diameter, versus flow rate are presented. In these figures and also on Figs. 14-17, flow rates are given in gallons per minute; the flow velocities have to be calculated. Based on the data available at this time, the mean velocity of the crossflow through the gaps between the tubes (designated the "B"-stream in the HTRI computer program) is 0.895 m/s (2.93 ft/sec) for a nominal flow rate of $0.063 \text{ m}^3/\text{s}$ (1000 gal/min) for the full tube bundle. For the most part, these curves depict subcritical tube vibration response up to the critical flow rate at which fluidelastic instability is initiated. In Figs. 14-17, the principal frequencies at which the tubes respond are presented for excitation provided by specific flow rates. These frequencies were obtained from the PSD curves of tube response.

Tubes V6 and V40 occupy similar positions near the shell periphery. Their response is somewhat similar too, even though the accelerometers were located in different tube spans. Figs. 10 and 11 show that the rms

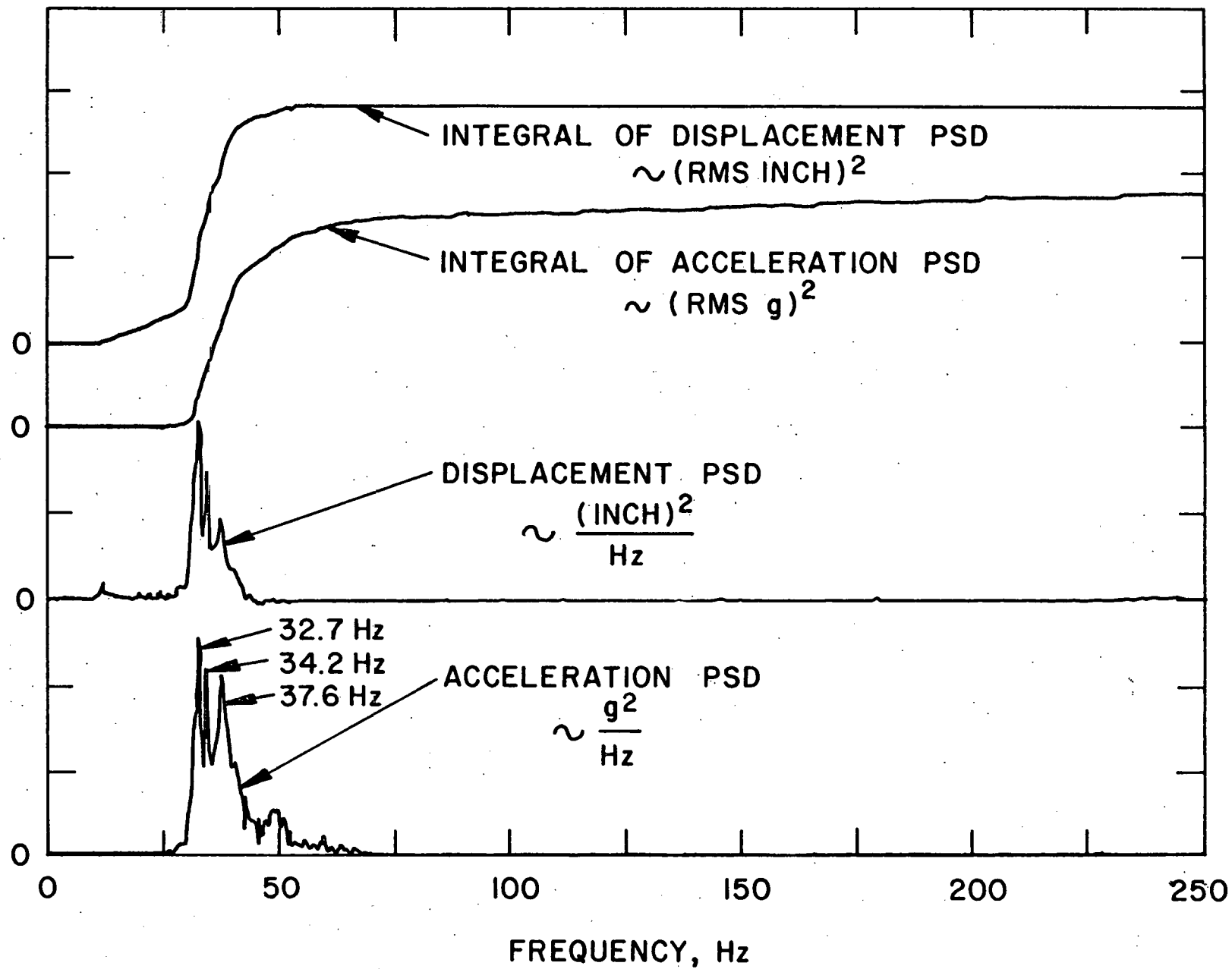


Fig. 9. Typical power spectral density (PSD) curves, Tube V6

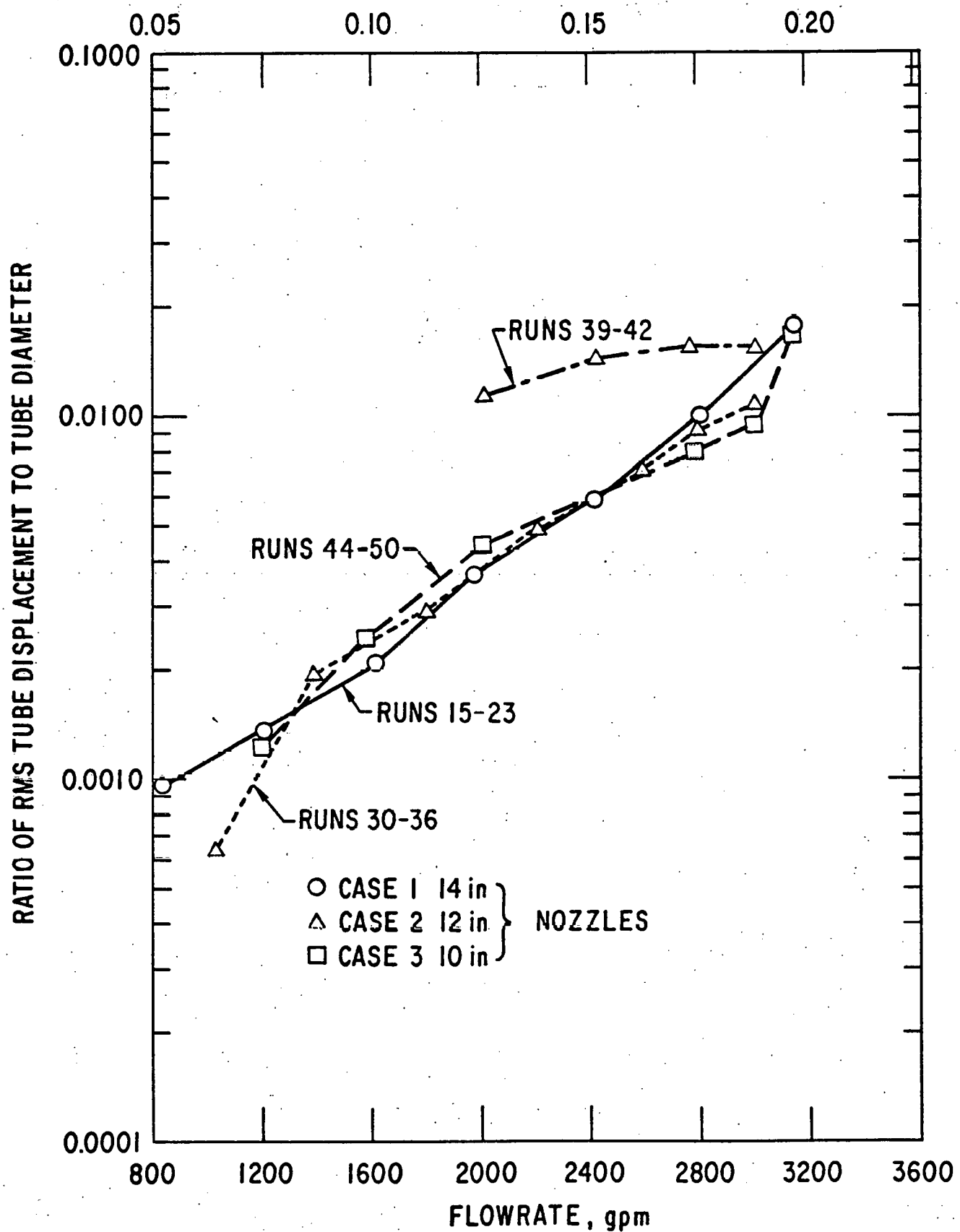
FLOWRATE, m^3/s 

Fig. 10. RMS displacement, Tube V6
(full tube bundle, 8 crosspass)

RATIO OF RMS TUBE DISPLACEMENT TO TUBE DIAMETER

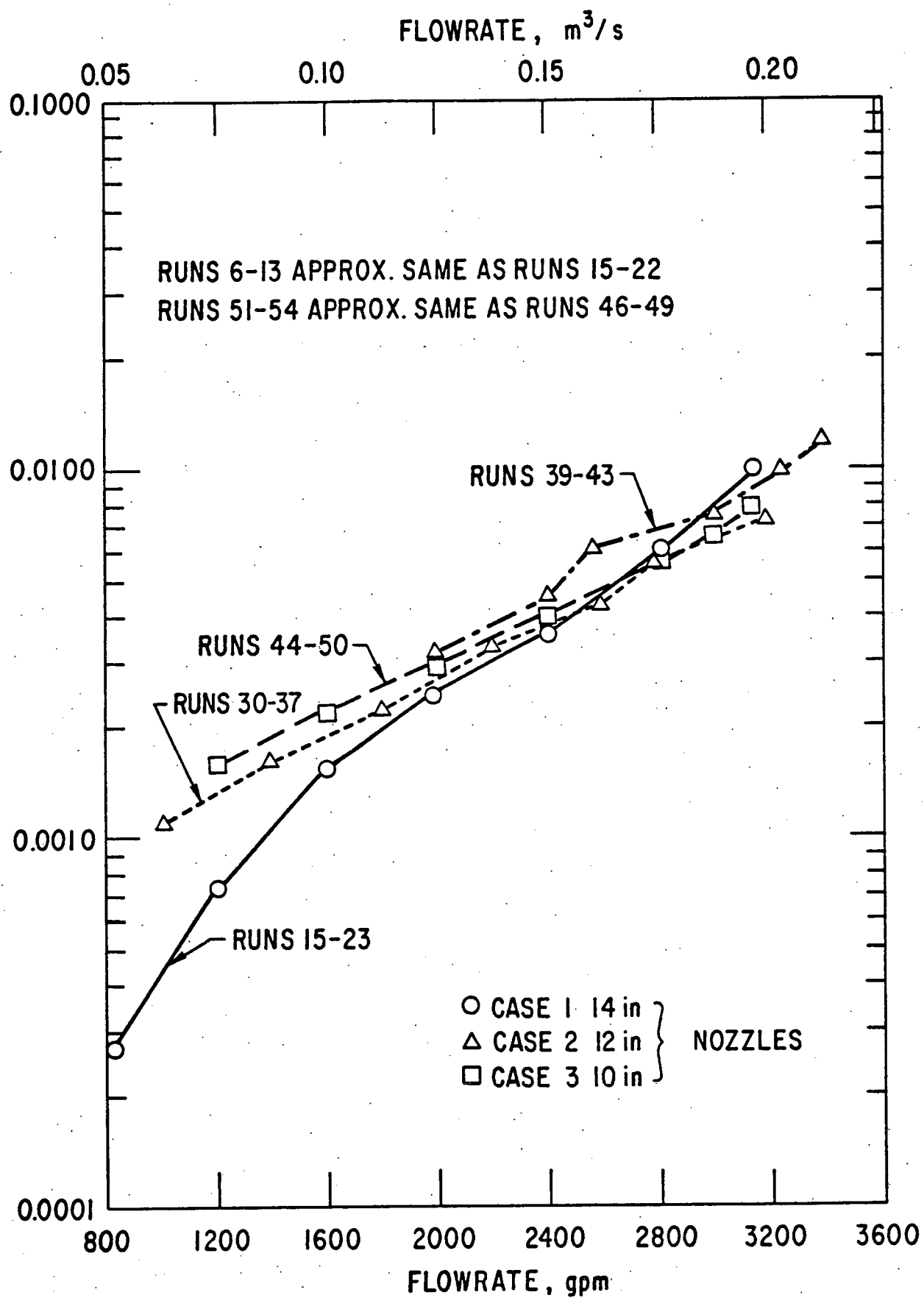


Fig. 11. RMS displacement, Tube V40
(full tube bundle, 8 crosspass)

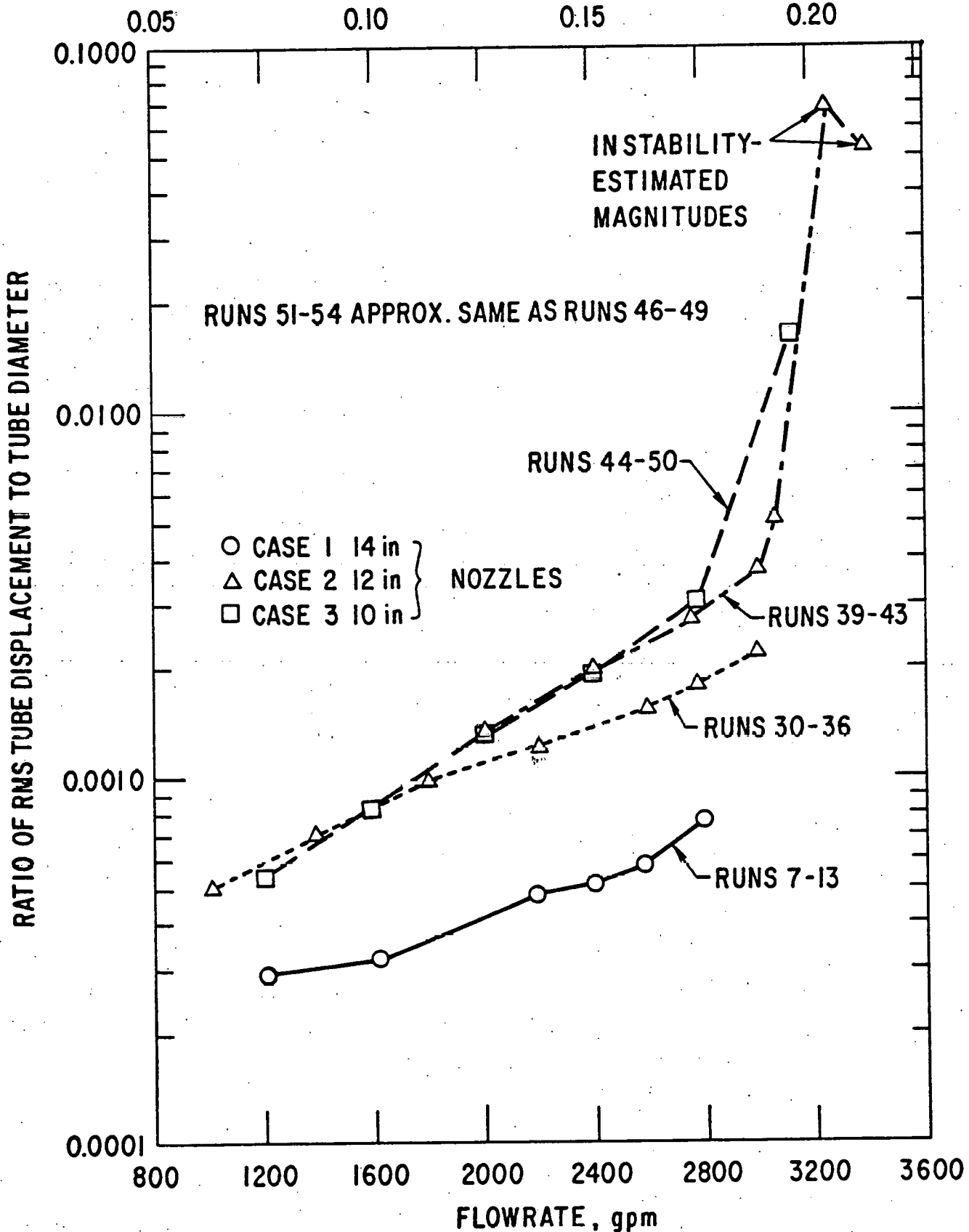
FLOWRATE, m^3/s 

Fig. 12. RMS displacement, Tube V24
(full tube bundle, 8 crosspass)

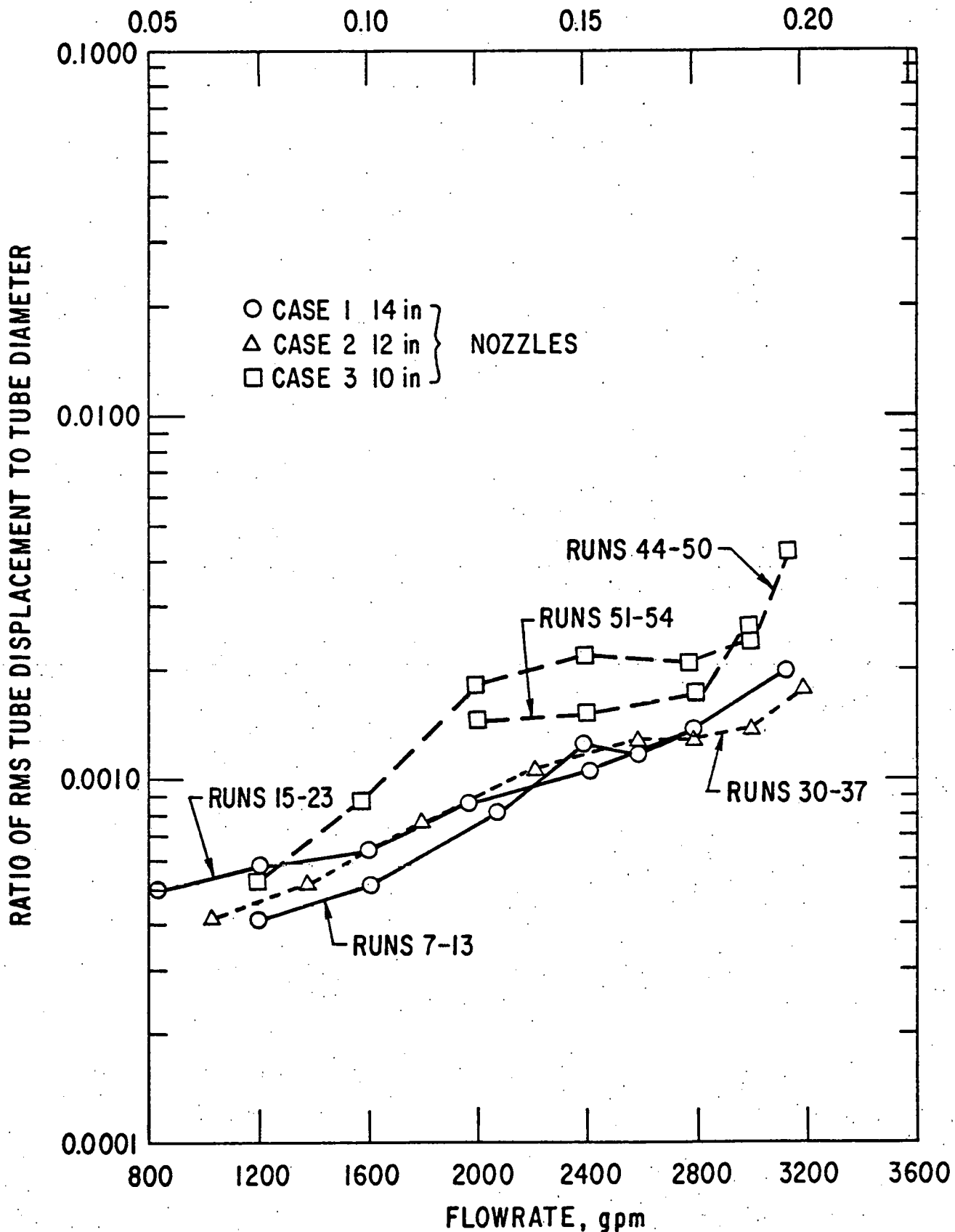
FLOWRATE, m^3/s 

Fig. 13. RMS displacement, Tube A23
(full tube bundle, 8 crosspass)

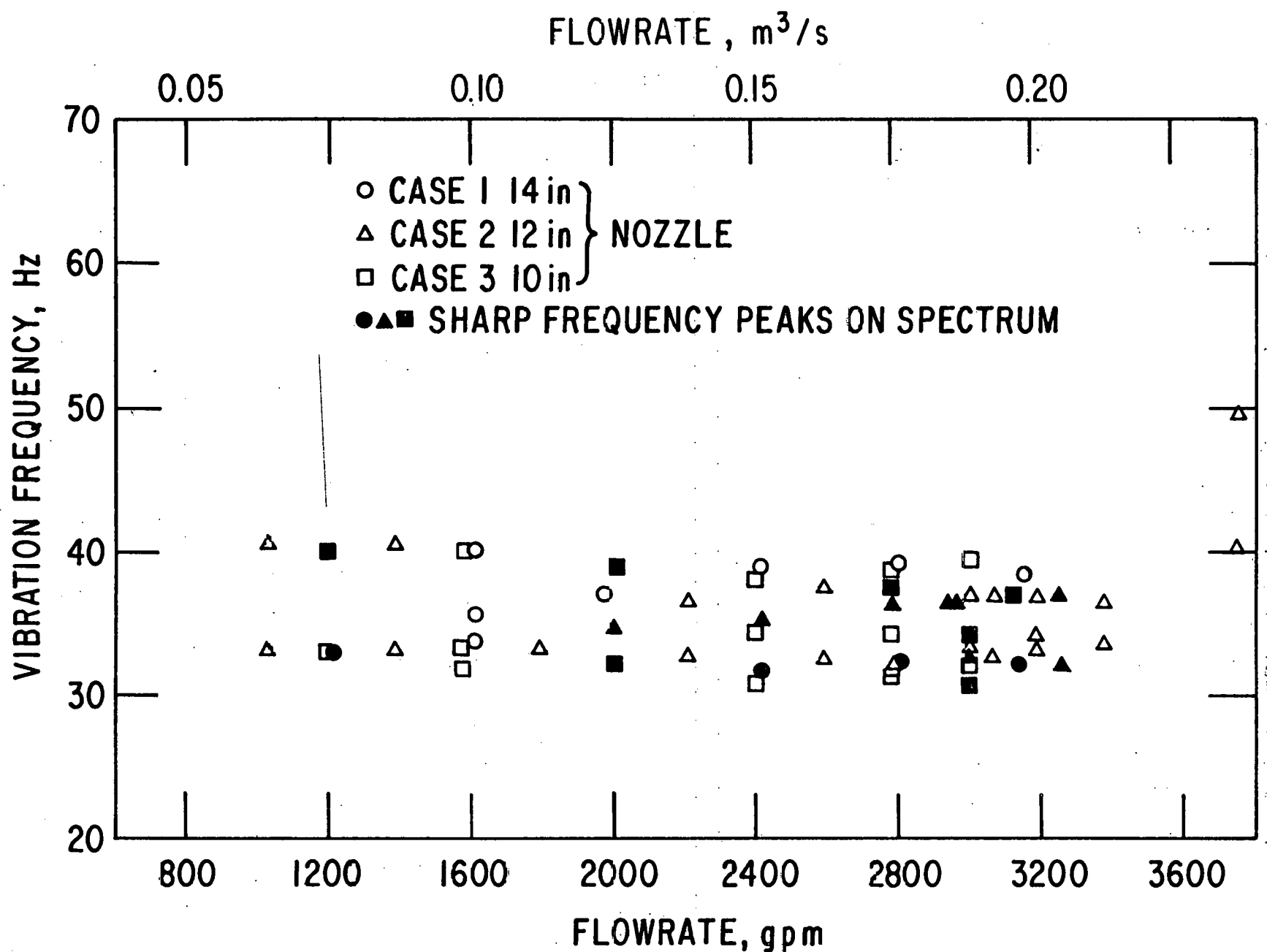


Fig. 14. Principal vibration frequencies, Tube V6
(full tube bundle, 8 crosspass)

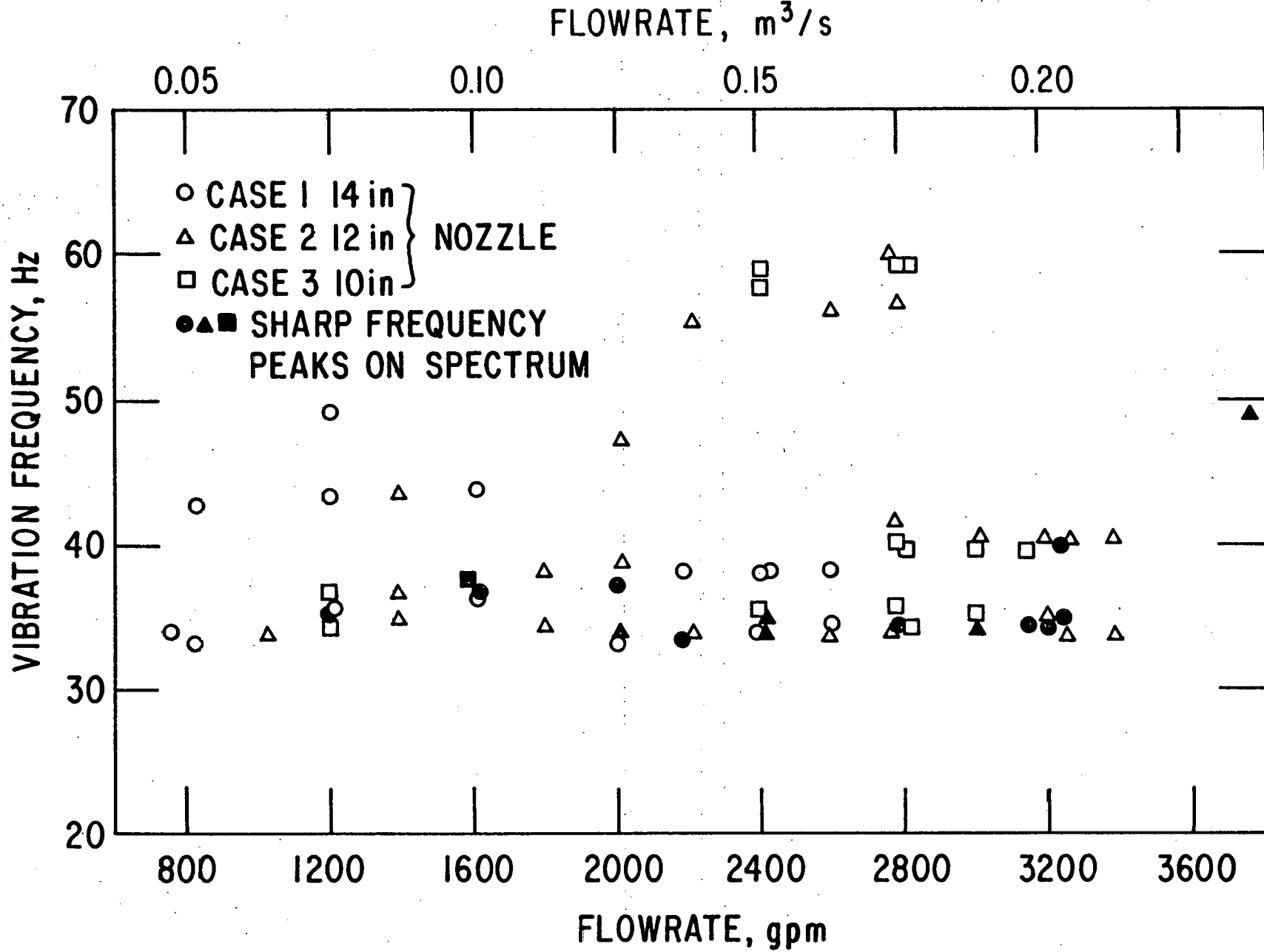


Fig. 15. Principal vibration frequencies, Tube V40
 (full tube bundle, 8 crosspass)

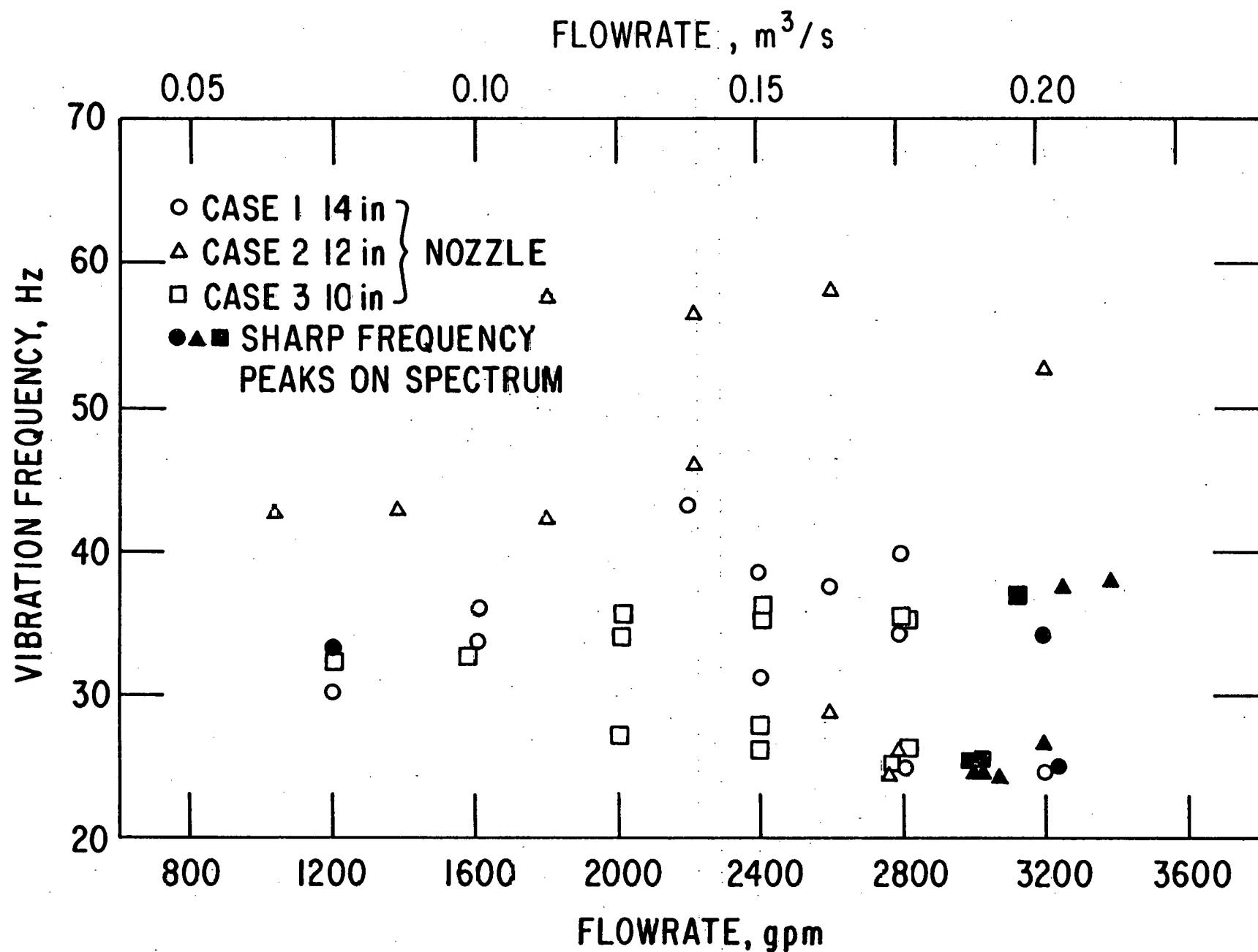


Fig. 16. Principal vibration frequencies, Tube V24
(full tube bundle, 8 crosspass)

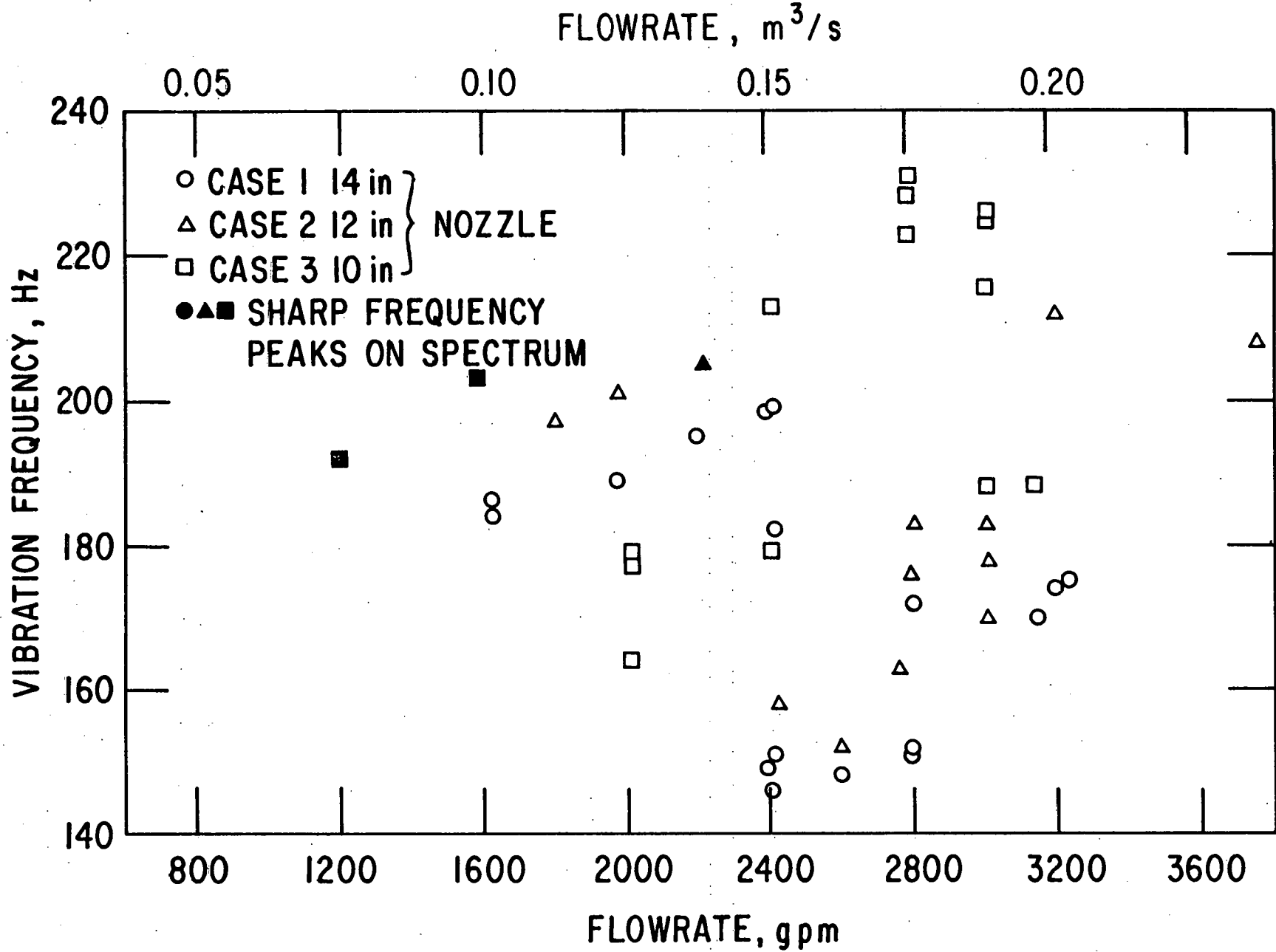


Fig. 17. Principal vibration frequencies, Tube A23
(full tube bundle, 8 crosspass)

amplitude increased by a factor of 10 as the flow rate was increased from 1000 gal/min to a value of 3250 gal/min, prior to instability. It is possible that these particular tubes were not physically impacting upon instability. The corresponding data, Figs. 14 and 15, indicate subtle changes of the fundamental natural frequency between about 32 and 36 Hz. In addition, a response at a frequency level about 4 to 6 Hz higher, presumably the second mode, is also generally observed.

As shown in Fig. 12, Tube V24 indicates the same general subcritical amplitude vs. flow rate trend. However, the displacement data of Fig. 12 for Runs 39-43, also serve to illustrate the abrupt increase in response that is experienced when the threshold flow rate is reached. It should be noted that the values of the magnitude of the large amplitude vibration are only estimated values. In general, displacement data from accelerometer signals obtained during tube impacting are not reliable. To improve reliability, efforts to work with cushioned accelerometers and an optical displacement tracker are continuing. The frequency data (Fig. 16) are fairly scattered; this tube also showed a 24 Hz component not observed on any other tube tested. A possible reason is that one of the baffles was not in contact and active as a support, but this could not be readily verified by simple theory.

Analysis of the acceleration signals from five-span tube A23 in the first row facing the inlet nozzle flow indicated generally a few distinct frequencies in the low frequency region, where the lowest three modes would be expected to be excited. More distinct excitation occurred at the higher frequencies, above 140 Hz. Fig. 17 indicates a scatter of frequencies in the range 140 to 240 Hz. The amplitude data on Fig. 13, based on double integration below 100 Hz, are to be viewed with discretion for reasons discussed previously. An interesting interaction occurred during Run 54 and

at other occasions when a specific excitation of tube A21 was particularly noted. Run 54 data show that without that interaction tubes A21 and A23 vibrated at frequencies of 187.5 and 225 Hz, respectively, both with an rms amplitude/diameter ratio of about 0.00003 at those frequencies. With the interaction both tubes A21 and A23 vibrated at 215 Hz with increased amplitude ratios of 0.0005 and 0.00007, respectively.

After most impacting tests, the tubes shaken severely enough to have slid in the O-rings or rotated were noted and usually moved back. Most of the tubes involved were in row V, but some of row W were often also effected. Examination of the disassembled four span tubes after the test indicated impacting marks on most tubes in rows V and W (Fig. 4). Tubes in the saddled row U indicated impacting marks about 20 to 22.5° above and/or below the flow direction plane, on the surfaces facing row V. In general, the instability, as evidenced by both a substantial increase in audible noise level and accelerometer response initiated at approximately 3250 gal/min for Cases 1 and 2 and, upon flow reduction, ceased at or slightly below that flow rate. For the five span tube the critical flow rate was about 3400 gal/min as indicated on Table 7.

For Case 3 tests with 10 inch diameter nozzle inserts the situation was more complex. As the flow rate was increased after Run 49 and again when formally performing scan Run 50, the instability initiated at 3130 gal/min (which was not exceeded) and did not cease until flow was reduced to 2380 gal/min. During scan Run 55, the central tubes in the row next to the row saddled in the baffle cut went into impacting vibration at 3250 gal/min. As the flow rate was increased, the tubes located in the region where the shell meets the baffle cut indicated impacting. At a still higher flow rate the five span tubes on the inlet/outlet side of the heat exchanger went into impacting as indicated in detail on Table 7. As the flow rate was reduced,

TABLE 7. Critical Flow Rates: Full Tube Bundle

Location of Tubes Affected (Refer to Fig. 4)	Flow Rate = (gal/min)		
	Inlet/Outlet Nozzle Size		
	14 inch (Case 1)	12 inch (Case 2)	10 inch (Case 3) Run 55
Start of instability (severe vibrations) upon increasing flow	Far window (opposite nozzles) - central region	3250	3190 [*]
	Far window - near shell periphery	3250	3190 ^{*+}
	Near window	≈ 3430	3760
Ceasing of severe vibrations upon flow reduction	Near window	-	3460
	Far window - near shell periphery	> 3100	> 3000
	Far window - central region	> 3100	> 3000
			1910 ^{***}

^{*} Run 37, tube V6; was 3250 for Run 43.

[†] Was 3510 for Run 37, tube V40.

^{**} Run 50, was 3250 for Run 55.

^{***} Was 2380 for Run 50.

Note: Computed crossflow velocity is 0.895 m/s (2.94 ft/sec) per 0.063 m³/s (1000 gal/min) flow rate.

the tubes went out of instability in the reverse order, with varying amounts of "hysteresis."

Case 3 results indicate that the high velocity central stream emerging from the 10 inch nozzle slightly increases the vibration potential of the centrally located tubes in the far window, at least compared to the ones near the shell periphery. But the probably more significant difference compared to the 14 and 12 diameter nozzle test is the substantially increased amount of hysteresis and the possible implications this may have for the stability of the bundle against transient disturbances.

Simple pitot tube traverses were conducted across the 14 inch diameter of the inlet nozzle, perpendicular to the plane of flow in the heat exchanger. This was done at two different flow rates. The results were rough and scattered, but indicated clearly that the maximum flow velocity did not occur in the pipe center, but at intermediate radial positions where the flow apparently speeded up in anticipation of the lowered resistance in the annular clearance space between the tube bundle in the shell.

High speed motion pictures taken into the ends of a cluster of back-lighted tubes during impacting turned out to be of fair quality, but not providing the excellent perception that was desired. This effort will be repeated with different equipment in the future.

B. No-Tubes-in-Window Configuration

The no-tubes-in-window configuration, described in Section II.D, contains only tubes supported or saddled on all seven baffles. The photograph of Fig. 5 indicates how the locations of four of the heavy stainless steel tie bolts and of four of the smaller sized tie bars (two of each are prominently visible on the photo) were now falling outside of the reduced perimeter of the bundle. These bolts and bars, unlike the others and the tubes, are supported only by every other baffle. Fig. 5 also indicates that the tie

bars, which hold the baffles in place and which were later observed to vibrate, do not extend into the first baffle crosspass (far end of picture) which comprises the inlet end zone exposed to the inlet flow entering from the nozzle.

The NTIW bundle was flow tested with nominal 10 inch and 14 inch inlet/exit nozzles designated Cases 4 and 5, respectively, and included in the listing on Table 5. During the flow test, five tubes (G15, H24, T24, U5, and U13) were instrumented with internal miniature accelerometers. As previously, a conventional accelerometer was installed on the shell (near pressure tap "B") and another on the tie bolt R14, sensitive in the axial direction. The test procedure was essentially the same as that used for the full tube bundle, the test history is presented on Table 8.

The test heat exchanger was exposed to flow rates up to 5030 gal/min. This corresponds to mean gap crossflow velocity of 4.70 m/s (15.4 ft/sec) based on a computer calculated 0.934 m/s (3.07 ft/sec) per 1000 gal/min relationship for the NTIW bundle. No large amplitude tube vibrations were observed even though some tubes were noticeably quivering. The power spectral density plot of the accelerometer signals usually indicated a broadband contribution above frequencies of 11.5 and 125 Hz for the tubes located, respectively, on and behind the bundle periphery. Only in a few instances one or two specific frequencies were prominently indicated. Rattling of undetermined origin was noticed to start at flow rates of about $0.11 \text{ m}^3/\text{s}$ (1800 gal/min). The two tie bars (front on Fig. 5) were observed through the observation port to vibrate significantly at flow rates of about 3000 gal/min. At the higher flow rates, the tie bar vibration subsided, and almost ceased at 5000 gal/min. Also, at those high flow rates, the heat exchanger appeared to run smoother, even though not necessarily quieter.

TABLE 8. Test History - NTIW Bundle

Test Date	Case	Run No.	Flow Rate (gal/min)	Comments
1/23/80	4	1	1180	
		2	1610	
		3	1970	
		4	2420	
		5	2810	
		6	3210	
		7	3620	
		8	3980	
		9	Scan	4000 - 1200 - 4000
2/4/80		10	4820	
		11	4330	
		12	3950	
		13	Scan	4000 - 5030
		14	5030	
2/8/80	5	15	1270	
		16	1580	
		17	2000	
		18	2400	
		19	2800	
		20	3190	
		21	3600	
		22	3990	
		23	4370	
		24	4800	
		25	5010	
		26	Scan	5000 - 1200
		27	Scan	1200 - 4000

VI. PRESSURE MEASUREMENTS

Pressure drop measurements were made during flow testing for all five of the heat exchanger configurations tested. The overall pressure drop is plotted for the various cases on Fig. 18. It was measured between the inlet and outlet taps designated A and I on Fig. 19. There were no significant differences between the measurements of Cases 1 and 2 as well as 4 and 5. Fig. 19 indicates the locations of the pressure taps labeled A through I on the shell, and also presents the normalized fractional distribution of the pressure drop, with the overall drop set equal to unity.

The dynamic signals obtained from the strain gage pressure transducer, mounted about 0.15 m (6 in.) downstream of pressure tap C, provided no data considered significant. The principal tube vibration frequencies were not prominent.

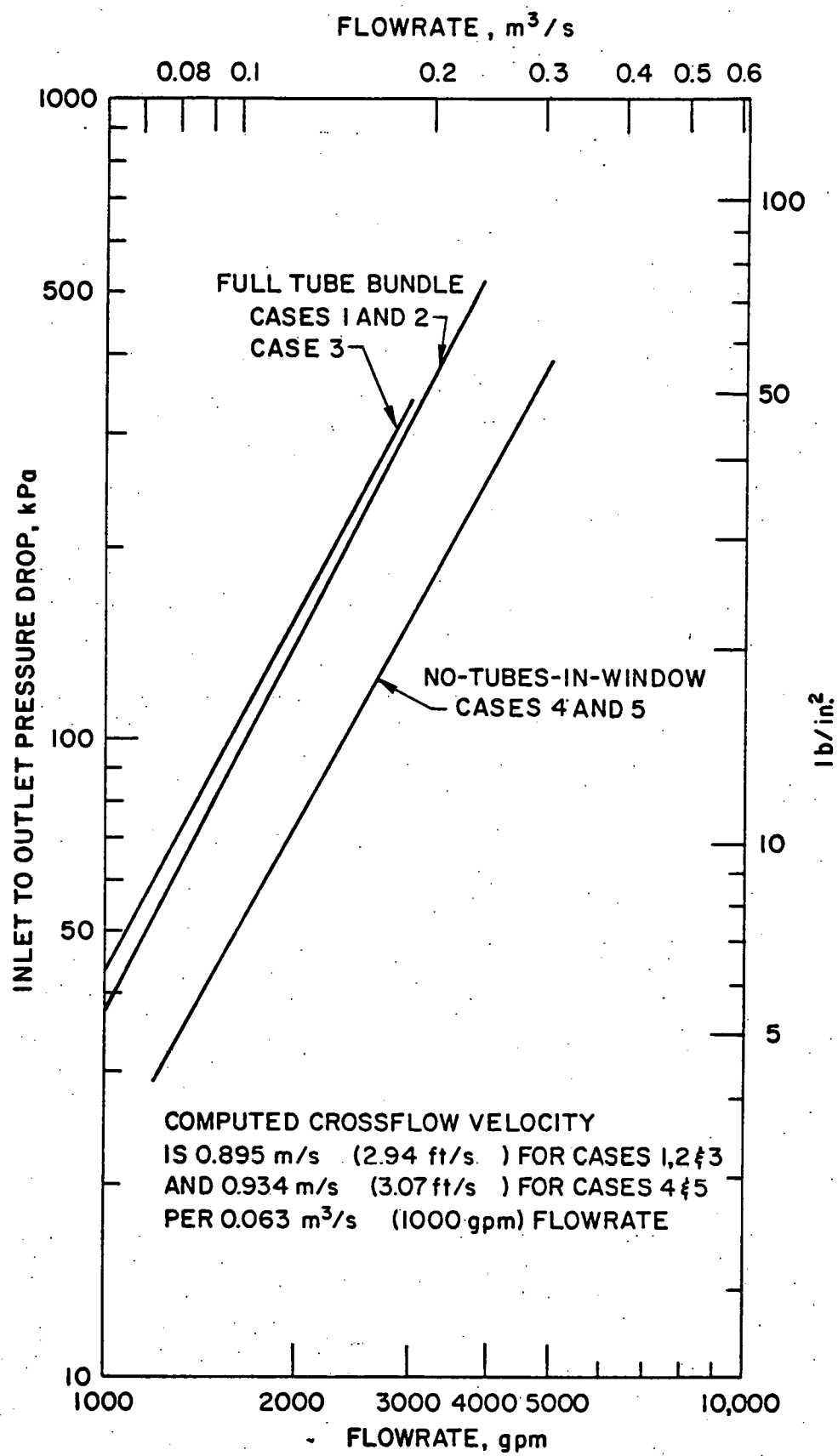
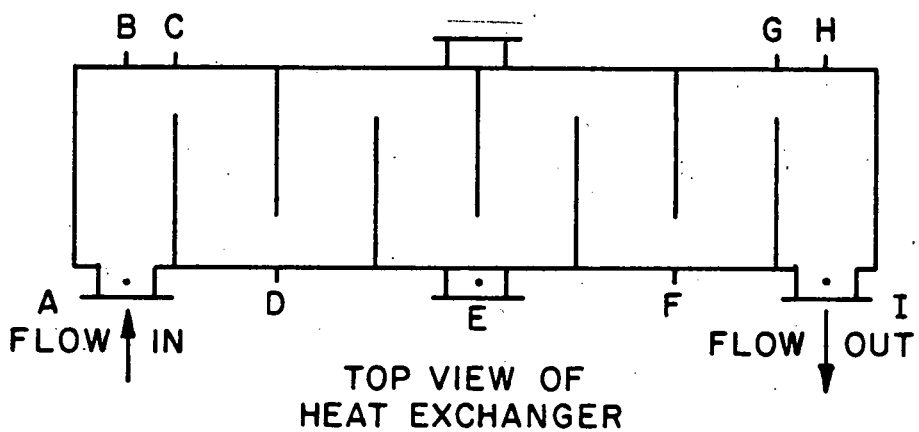


Fig. 18. Heat exchanger pressure drop (8 crosspass configuration)



TAPS A, E, AND I ON BOTTOM OF NOZZLE.
TAPS B,C,D,F,G, AND H ON SHELL IN PLANE OF FLOW

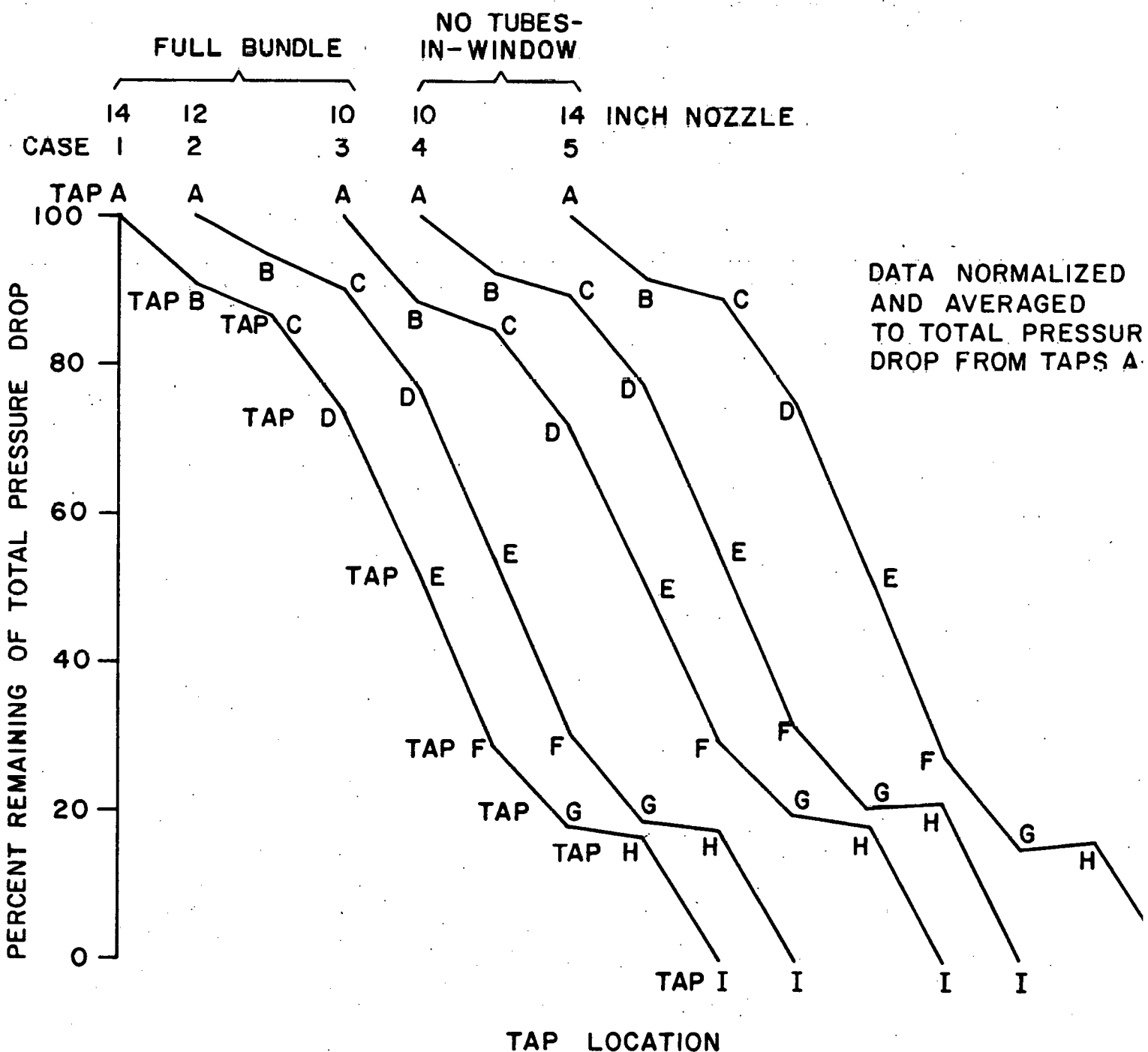


Fig. 19. Tap location and pressure drop distribution

VII. CONCLUDING REMARKS

The study is motivated by the need to obtain tube vibration data from an actual heat exchanger, as well as from field experiences, for use in evaluating and improving existing prediction methods. Not unexpectedly, the dynamic response of tubes in an actual unit proved to be extremely complex. The complexities are associated with the tubes not being perfectly straight, relatively small tube/baffle hole clearances, the very large number of tube/baffle interfaces, and nonuniform flow. Lack of tube straightness coupled with small tube/baffle hole clearances implies that at the many tube/baffle interfaces the tube support condition may vary from one of preload against the baffle to a floating condition in which the tube is centered in the baffle hole. These conditions can be expected to vary with operating conditions as the shellside flow induces a steady drag force on the tubes in the flow direction. Such changes in support conditions can be expected to effect damping and, to a lesser degree, frequencies and mode shape. The problem is compounded by the large number of tubes and the practical difficulty in not being able to instrument all tubes. However, it was possible to identify groups of tubes in specific locations in the tube bundle that were most susceptible to vibration and that were among the first to experience fluidelastic instability.

At intermediate flow rates, and as the flow rate was increased, rattling of the tubes within their baffle supports was detected on accelerometer signals and audibly. The rattling would come and go as flow rate was increased. There are many factors that can influence rattling, one of the less obvious ones is the steady state pressure drop, that may actually "seat" a tube at higher flow rates and stop rattling there. Many commercial heat exchangers are said to be operating satisfactorily with moderate rattling; however, instances of failure, sometimes after many years of service, have

been reported. It appears that more needs to be known about the consequence of rattling.

The onset of fluidelastic instability was easily detected by the abrupt increase in audible noise coming from the unit. From the noise alone it is easy to understand how units can shake themselves apart in a very short period of time. Onset of instability could also be determined from the accelerometer signals. While the critical flow rate could be readily established, the determination of which tubes were undergoing large amplitude motions and impacting was not so easily made. Because of coupling through the water and structure one could not be certain that a particular tube was impacting just because the accelerometer in that tube indicated an impacting condition. Some insight could be gained by backlighting the tube bundle and visually noting which tubes were vibrating the most. A more positive indication was fortuitously provided by the fact that the tubes undergoing large motion would rotate and move axially thus allowing easy identification from the end of the bundle. By this method it was determined that the four-span tubes in the row adjacent to the row saddled in the baffle cut and in the region where the baffle cut meets the shell experienced fluidelastic instability.

Since the heat exchanger is complex with respect to structure and flow field, the test results indicated some subtle and some not so subtle changes from test to test as reflected in the scatter of data seen on Figs. 10-17. Nevertheless, the critical flow rate associated with fluidelastic instability of the full tube bundle configuration was reasonably repeatable. Inlet/outlet nozzle sizes did not have much influence on the critical flow rate as flow was increased; however, once triggered, the tube bundle exposed to the 10 inch nozzles did not recover from the instability until the flow was reduced much below the levels sufficient for the 12 and 14 inch nozzle

tests as indicated on Fig. 7. At this time no explanation can be offered for this phenomenon; this will be of interest during future test work.

The use of tube vibration data, obtained from the test heat exchanger, to evaluate and improve state-of-the-art prediction methods is the objective of future work. Nevertheless, it is of interest to preliminarily evaluate the applicability of the currently used criterion for estimating the onset of fluidelastic instability. The fluidelastic mechanism of interest was first reported by Connors [7]: A tube array becomes unstable and vibrates with large amplitude motion when, for a given tube motion, the energy input from the flow exceeds the energy dissipated through damping. For an idealized tube bundle exposed to uniform crossflow, the critical flow velocity above which large amplitude tube vibrations occur is characterized by

$$\bar{U}_{cr} = \frac{U_{cr}}{fD} = K \left(\frac{m_v \delta}{\rho D^2} \right)^{1/2} \quad (1)$$

where

\bar{U}_{cr} = reduced velocity (reciprocal Strouhal number)

U_{cr} = critical mean flow velocity in gap between adjacent tubes

f = tube natural frequency

D = tube outside diameter

m_v = virtual mass per unit length of tube

$\delta = 2\pi\zeta$ = log decrement of damping

ρ = density of shellside fluid

K = instability threshold constant depending, in part, on the layout of the tube pattern.

For a particular tube bank, Eq. (1) can be solved for the critical flow velocity, U_{cr} ; the tubes will be stable or unstable when the actual crossflow velocity U is lower or higher, respectively, than U_{cr} .

Solution of Eq. (1) requires knowledge of the mean flow velocity in the transverse gap, damping, tube natural frequency, and instability constant. There are difficulties associated with the establishment of each of these parameters. In particular, for the case of multi-span tube arrays and significant spanwise variations in flow velocities, as generally occur in real heat exchangers, it is necessary to consider an effective flow velocity for each mode [8,9], obtained by weighting the crossflow velocity with the mode shape and integrating over the span length. In certain heat exchanger applications, spanwise variations in density can also occur and in such cases should be treated in a similar manner. Damping is difficult to measure and generally can be expected to be a function of flow rate and vibration amplitude, and to vary from tube to tube. With regard to frequency and mode shape, fluid-structure coupling together with the multi-span condition results in bands of closely spaced frequencies; it is often difficult to determine a priori in which mode the instability will occur.

In applying Eq. (1) to the full tube bundle configuration of the test heat exchanger, it should be noted that, in the absence of measured values of flow velocity, mean flow velocity was computed from measured flow rate; only very rough estimates of equivalent viscous damping factors were possible; and a typical tube vibration frequency was assumed. Data from Run 50, performed with 10 inch inlet/outlet nozzles, provide

$U_{cr} = 2.80 \text{ m/s (9.20 ft/sec) mean gap flow velocity (calculated)}$

based on $0.197 \text{ m}^3/\text{s (3130 gal/min) measured loop flow rate,}$

$f = 37.1 \text{ Hz, typical tube vibration frequency,}$

and $D = 19.05 \text{ mm (0.625 ft) tube diameter,}$

resulting in

$$\bar{U}_{cr} = 3.96 .$$

This is the lowest critical reduced velocity encountered for the 8 crosspass, full tube bundle; based on the generally observed critical flow rate of 3250 gal/min (Table 7) and a natural frequency of 32.2 Hz determined in still water, a

$$\bar{U}_{cr} = 4.74 ,$$

would have been obtained. For the subject tests, the mass of the tube (m_{tube}) is 0.597 kg/m (0.0335 lb/in.), which, with the added mass of the displaced water multiplied by a factor of 2.97, provides

$$m_v = 1.44 \text{ kg/m (0.0808 lb/in.)}.$$

With $\delta = 0.22$, based on $\zeta = 0.035$, and

$$\rho = 10^3 \text{ kg/m}^3 (0.0361 \text{ lb/in.}^3),$$

the damping parameter $m_v \delta / \rho D^2 = 0.875$. Using $\bar{U}_{cr} = 3.96$ to solve Eq. (1) for the instability constant obtains

$$K = 4.23 .$$

Within the scope of this analysis, this value of K is considered to be low and conservative because input values of m_v and δ were taken on the high and \bar{U}_{cr} on the low side, respectively. It is of interest to note that this value of K agrees favorably with the value of 3.3 recommended by Pettigrew et al. [9] as a guideline for vibration analysis which allows a realistic safety margin.

The NTIW bundle was exposed to flow rates up to 5030 gal/min, providing a computed crossflow velocity of 4.70 m/s (15.4 ft/sec). However, with a natural tube frequency (e.g., $f = 119$ Hz) much higher than that of the tubes in the window of the full bundle, the highest reduced flow velocity that could be imposed was

$$\bar{U} = 2.07 ,$$

not sufficient to induce a flow instability of the tubes.

The data presented here are not necessarily final; it is hoped that the planned evaluation of test and field experience data, possibly in conjunction with more improved relationships by the researchers in the field, will provide better insights in the future.

In closing, this effort has, within the limits of the experiments performed, provided the following:

- Versatile test heat exchanger available for tube vibration testing
- Observation of tube rattling in baffles initiated at about half of critical flow rate
- Critical flow rate determined for full tube bundle configuration
- Critical flow rate shown to be not much influenced by nozzle size when flow was measured
- Small nozzle size resulted in "hysteresis" as flow was reduced
- No-tubes-in-window configuration did not become unstable within reasonable flow rates tested
- Isolated tie bars of NTIW bundle can vibrate
- Pressure drop distribution data determined are considered important for computer program input/evaluation
- Preliminary determination of fluidelastic instability threshold constant showed to be in good agreement with recommended design practice

In addition,

- Data bank of field experience data was initiated [2]
- Program staff established contact with heat exchanger industry.

ACKNOWLEDGMENTS

This work was performed under the sponsorship of the United States Department of Energy, Division of Fossil Energy (USDOE/FE) and represents a U.S. contribution to the International Energy Agency (IEA) Program of Research and Development on Energy Conservation in Heat Transfer and Heat Exchangers. Drs. W. H. Thielbahr and M. Perlsweig of the USDOE were instrumental in the early definition and establishment of this effort. The program is currently one of a group of Heat Exchanger Technology Projects being managed by the USDOE's Pittsburgh Energy Technology Center (PETC); Dr. J. D. Hickerson is the Project Manager at PETC.

The authors gratefully acknowledge the assistance of D. M. Engel and M. J. Featherstone in the setup and conduct of the test; J. Kissel and D. Fijas of American Standard, Buffalo, New York, for consultation on the design of the test heat exchanger and cooperation during fabrication; and Drs. J. M. Chenoweth and J. Taborek of HTRI for consultation on the heat exchanger design, selection of test parameters, and analysis and interpretation of test data.

REFERENCES

1. Chenoweth, J. M., "Flow-Induced Tube Vibrations in Shell and Tube Heat Exchangers," ERDA Report SAN/1273-1 (February 1977).
2. Halle, H., Chenoweth, J. M., and Wambsganss, M. W., "DOE/ANL/HTRI Heat Exchanger Tube Vibration Data Bank," ANL Technical Memorandum ANL-CT-80-3 (February 1980).
3. Chung, H. H., "Analysis Method for Calculating Vibration Characteristics of Beams with Intermediate Supports," ANL Technical Memorandum ANL-CT-79-41 (July 1979).
4. Shin, Y. W., Jendrzejczyk, J. A., and Wambsganss, M. W., "Vibration of a Heat Exchanger Tube with Tube/Support Impact," ASME Paper No. 77-JPGC-NE-5 (1977).
5. Collinson, A. E., and Warneford, I. P., "Vibration Tests of Single Heat Exchanger Tubes in Air and Static Water," paper to be published in Proceedings of International Conference on Vibration in Nuclear Plants, Keswick, England (1978).
6. Chen, S. S., "Dynamics of Heat Exchanger Tube Banks," ASME Paper No. 76-WA-FE-28 (1976).
7. Connors, H. J., Jr., "Fluidelastic Vibration of Tube Arrays Excited by Cross Flow," Proceedings of the Symposium on Flow-Induced Vibration in Heat Exchangers, ASME Winter Annual Meeting, New York, Dec. 1, 1970, pp. 42-56.
8. Connors, H. J., Jr., "Fluidelastic Vibration of Heat Exchanger Tube Arrays," ASME Paper No. 77-DET-90 (1977).
9. Pettigrew, M. J., Sylvestre, Y., and Campagna, A. O., "Vibration Analysis of Heat Exchanger and Steam Generator Designs," Nucl. Eng. Des. 48, 97-115 (1978).

APPENDIX A

Principal Test Instrumentation

- Turbine flow meters
Foxboro
- Flow rate reading units
Flow Technology
Programmable rate indicators, Model PRI-3
- Differential pressure transducers
Viatran, Model 209
Pressure range: \pm 50 psid bidirectional
- Digital transducer indicator (used with differential pressure transducer)
Doric, Series 420
- Miniature accelerometers, internal-to-tube mounted
Endevco, Model 22
- Externally mounted accelerometers
Endevco, Model 2271A
- Charge amplifiers
Endevco, Model 2735
- Subminiature dynamic pressure transducers
Sensotec, Type K
Pressure range 0-200 psia
- Bridge conditioner
Unholtz-Dickie, Model No. D22
- Fast Fourier transform analyzer
Hewlett Packard, Model 5451B
- Tape recorder
Ampex PR-3000

APPENDIX B

Preparatory Test Work

During the early phases of the program when the test heat exchanger was in the design and fabrication stages, exploratory bench tests were performed to determine the in-air natural frequencies and damping of a 19.1 mm (0.75 in.) O.D. near prototypic tube, which was mounted with O-rings in simulated tubesheets spaced about 2 m (80 in.) apart and supported by a midspan baffle. The purpose of these tests was a) to verify that the O-ring mounting system provided tube frequency response that corresponded to clamped rather than simply supported end conditions and b) to investigate the effect of baffle hole clearance on the tube natural frequency.

The frequency response of the tubes was determined at three different excitation input power levels. The tests were conducted with various central simulated baffles providing different tube to baffle-hole clearances. The test results were as follows: The natural frequencies were found to be near the values calculated from clamped end conditions. The natural frequencies decreased slightly with increasing excitation, i.e., vibration amplitude levels, and, generally, also with increasing tube/baffle clearances. At the fundamental natural frequency, the equivalent viscous damping ratio was approximately 0.03. During tests with large clearances, vibrations at a frequency characteristics of a single span, i.e., no central support, were evident.